Table of Contents

Page

List of Tables

List of Figures

Chapter II-7
Harbor Hydrodynamics

II-7-1. Introduction

a. A harbor is a sheltered part of a body of water deep enough to provide anchorage for ships or a place of shelter; refuge. The purpose of a harbor is to provide safety for boats and ships at mooring or anchor and to provide a place where upland activities can interface with waterborne activities. Harbors range in complexity from the basic harbor of refuge, consisting of minimal or no upland support and only moderate protective anchorage from storm waves to the most complex, consisting of commercial port facilities, recreational marinas, and fuel docks linked to the sea through extensive navigation channels and protective navigation structures. Key features of all harbors include shelter from both long- and short-period open ocean waves, easy and safe access to the ocean in all types of weather, adequate depth and maneuvering room within the harbor, shelter from storm winds, and minimal navigation channel dredging.

b. Harbors can be classified according to location relative to the shoreline or coast. Figure II-7-1 illustrates six harbor classifications. The inland basin and offshore basin require considerable construction, including protective navigation structures and harbor and channel dredging to provide adequate protection. They are usually constructed where no natural features exist but where a facility is required. Examples of such harbors are Port Canaveral, Florida, Marina del Rey, California (inland basin), and Gulfport, Mississippi.

c. The natural geography can provide partial protection or headlands that can be augmented to construct a protective harbor. This approach may reduce the initial costs of construction. Examples of such harbors are Half Moon Bay Harbor, California; and Barcelona Harbor, New York (bay indentation); Crescent City Harbor, California; and Palm Beach Harbor, Florida (offshore island).

d. In some locations, the land can provide protective harbors requiring minimal modification. Examples include inside estuaries and up rivers such as at Panama City Harbor, Florida; Kings Bay, Georgia, (natural harbor); Port of Portland, Oregon; and New Orleans, Louisiana (river harbor).

e. The U.S. Army Corps of Engineers has constructed hundreds of harbor projects that include protective structures such as breakwaters, jetties, and navigation channels. Projects are classified by depth and range from deep-draft projects with navigation channel depths greater than -45 ft, to intermediate-depth projects with depths between -20 ft and -45 ft, to shallow-draft projects with depths less than -20 ft. Currently, USACE operates and maintains over 25,000 miles of navigation channels in association with hundreds of harbor projects.

f. This chapter covers basic harbor hydrodynamics. Harbor design is covered in Part V. The chapter covers wave diffraction, wave transmission and reflection, harbor oscillations, flushing and circulation, and vessel interactions. These are important elements that must be understood in order to design a safe harbor that is operationally efficient.

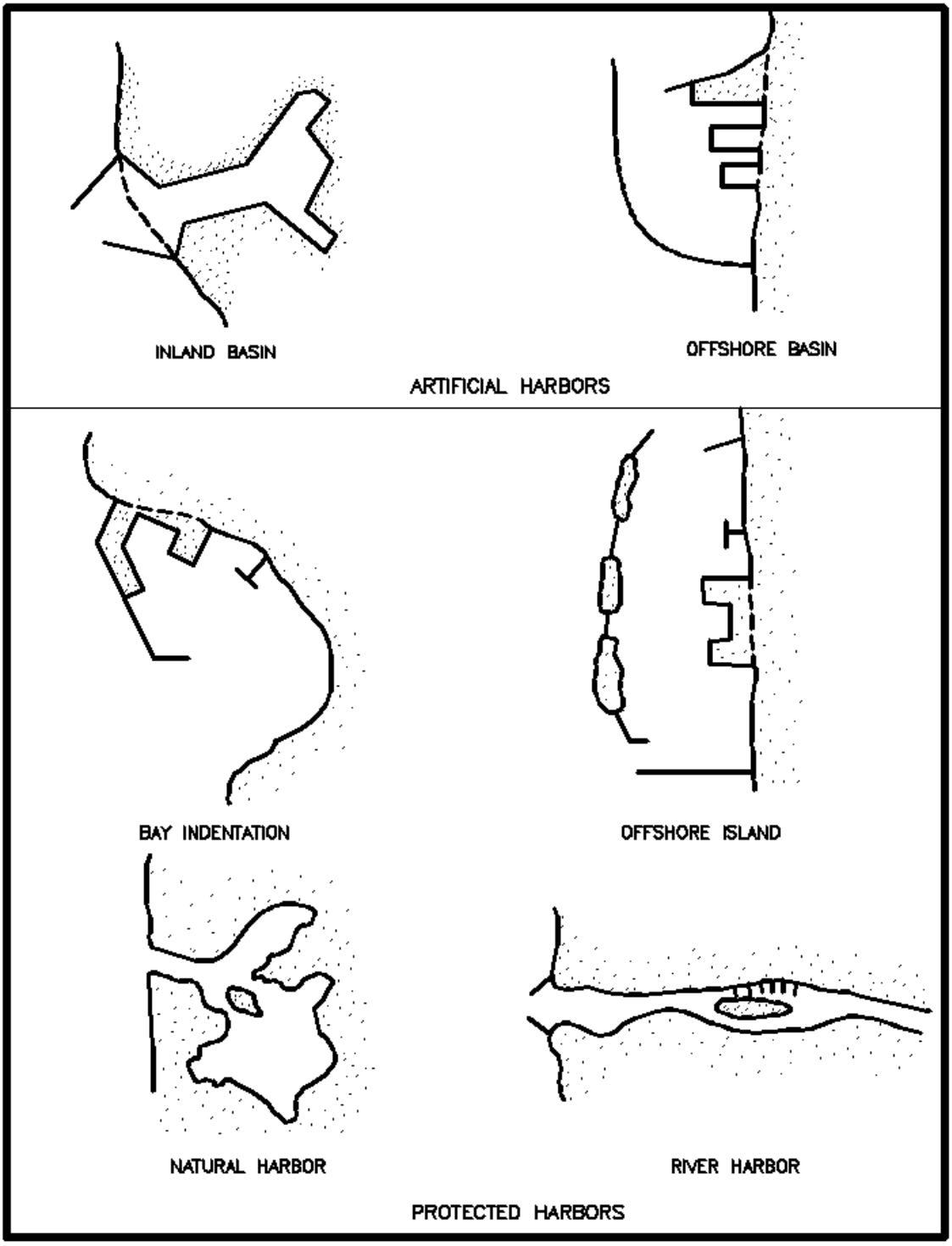

Figure II-7-1. Harbor siting classifications

II-7-2. Wave Diffraction

a. Definition of diffraction.

(1) Consider a long-crested wave that has a variable height along its crest. As this wave propagates forward, there will be a lateral transfer of wave energy along the crest (perpendicular to the direction of wave propagation). The energy transfer will be from points of greater to lesser wave height. This process is known as wave diffraction.

(2) Nearshore wave refraction will cause concentrations of wave energy at points where wave orthogonals converge. Diffraction will lessen this refraction-induced energy concentration by causing wave energy to transfer across the orthogonals away from the region of concentration. Consequently, wave diffraction can have a small effect on the resulting heights of waves that approach harbor entrances.

(3) Diffraction has a particularly significant effect on wave conditions inside a harbor. When waves propagate past the end of a breakwater, diffraction causes the wave crests to spread into the shadow zone in the lee of the breakwater. The wave crest orientations and wave heights in the shadow zone are significantly altered.

b. Diffraction analysis.

(1) Much of the material developed for wave diffraction analysis employs monochromatic waves. Ideally, an analysis should employ the directional spectral conditions. But, for a preliminary design analysis, one or a set of monochromatic wave diffraction analyses is often used to represent the more complex result that occurs when a directional spectrum of waves diffracts at a harbor.

(2) In the material presented below, monochromatic results are presented first. Then, some of the available results for diffraction of irregular waves are presented. These results are based on the superposition of several monochromatic waves having a range of representative frequencies and directions. This type of analysis requires significant effort, but it can be carried out where the situation so requires. Also, physical model tests employing a directional wave spectrum can be used for a harbor diffraction analysis.

c. Diffraction at a harbor entrance. A major concern in the planning and design of coastal harbors is the analysis of wave conditions (height and direction) that occur inside the harbor for selected incident design waves. These waves may shoal and refract after they pass through the harbor entrance; but, the dominant process affecting interior wave conditions is usually wave diffraction. Two generic types of conditions are most commonly encountered: wave diffraction past the tip of a single long breakwater and wave diffraction through a relatively small gap in a breakwater.

(1) Waves passing a single structure.

(a) Figure II-7-2 shows a long-crested monochromatic wave approaching a semi-infinite breakwater in a region where the water depth is constant (i.e. no wave refraction or shoaling). A portion of the wave will hit the breakwater where it will be partially dissipated and partially reflected. The portion of the wave that passes the breakwater tip will diffract into the breakwater lee. The diffracted wave crests will essentially form concentric circular arcs with the wave height decreasing along the crest of each wave. The region where wave heights are affected by diffraction will extend out to the dashed line in Figure II-7-2.

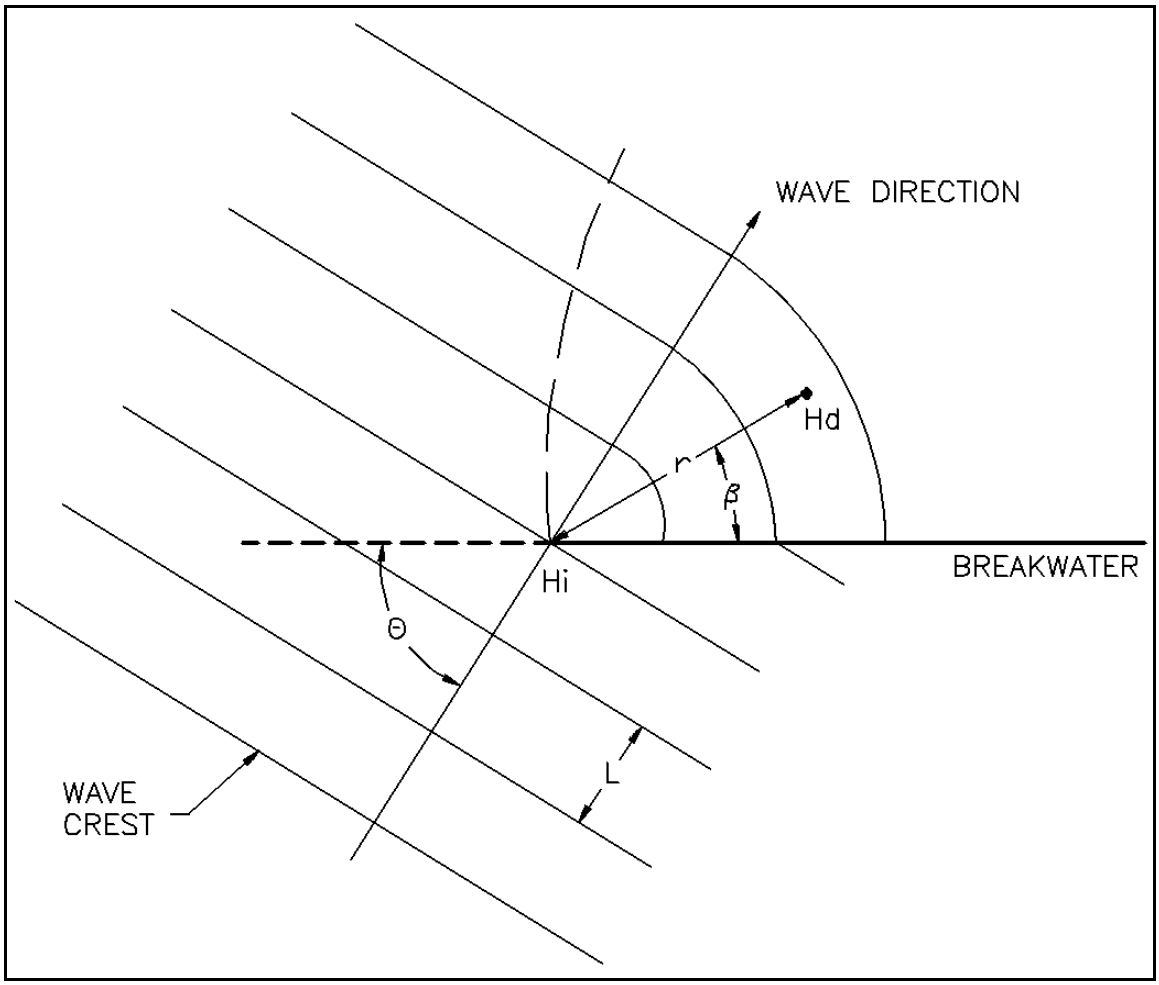

Figure II-7-2. Wave diffraction, definition of terms

(b) The reflected wave crests (not shown in the figure) would also diffract to form concentric wave crests that curl around the breakwater tip into the lee. These waves are typically much lower than the incident waves and are more affected by diffraction when they reach the breakwater lee, so they typically have a very small height in the lee of the breakwater.

(c) A diffraction coefficient $K' = H_d/H_i$ can be defined where H_d is the diffracted wave height at a point in the lee of the breakwater and H_i is the incident wave height at the breakwater tip. If r is the radial distance from the breakwater tip to the point where K' is to be determined and β is the angle between the breakwater and this radial, then $K' = fcn(r/L, \beta, \theta)$ where θ defines the incident wave direction (see Figure II-7-2) and L is the wave length. Consequently, for a given location in the lee of the breakwater, the diffraction coefficient is a function of the incident wave period and direction of approach. So, for a spectrum of incident waves, each frequency component in the wave spectrum would have a different diffraction coefficient at a given location in the breakwater lee.

(d) The general problem depicted in Figure II-7-2 was originally solved by Sommerfeld (1896) for the diffraction of light passing the edge of a semi-infinite screen. Penny and Price (1952) showed that the same solution applies to the diffraction of linear surface waves on water of constant depth that propagate past the end of a semi-infinite thin, vertical-faced, rigid, impermeable barrier. Thus, the diffraction coefficients in the structure lee include the effects of the diffracted incident wave and the much smaller diffracted wave that

reflects completely from the structure. Wiegel (1962) summarizes the Penny and Price (1952) solution and tabulates results of this solution ($K' = fct(r/L, \beta, \theta)$ for selected values of r/L, β and θ. Figure II-7-3 shows Wiegel's (1962) results for an approach angle θ of 60 deg. Plots of approach angles θ varying by 15-deg intervals from 15 to 180 deg can be found in Wiegel (1962) and the *Shore Protection Manual* (1984).

(e) An interesting feature demonstrated by Figure II-7-3 is that for this approach angle, the value of the diffraction coefficient along a line in the lee of the breakwater that extends from the breakwater tip in the direction of the approaching wave is approximately 0.5. This is true not only for the approach angle of 60 deg, but for any approach angle. Note also that for a given location in the lee of a breakwater, a one-dimensional spectrum of waves that comes from the same direction will undergo a greater decrease in height(energy density) for successively higher frequency waves in the spectrum. Increasing frequencies mean shorter wavelengths and consequently larger values of r/L (for given values of β and θ). Thus the diffracted spectrum will have a shift in energy density towards the lower frequency portion of the spectrum.

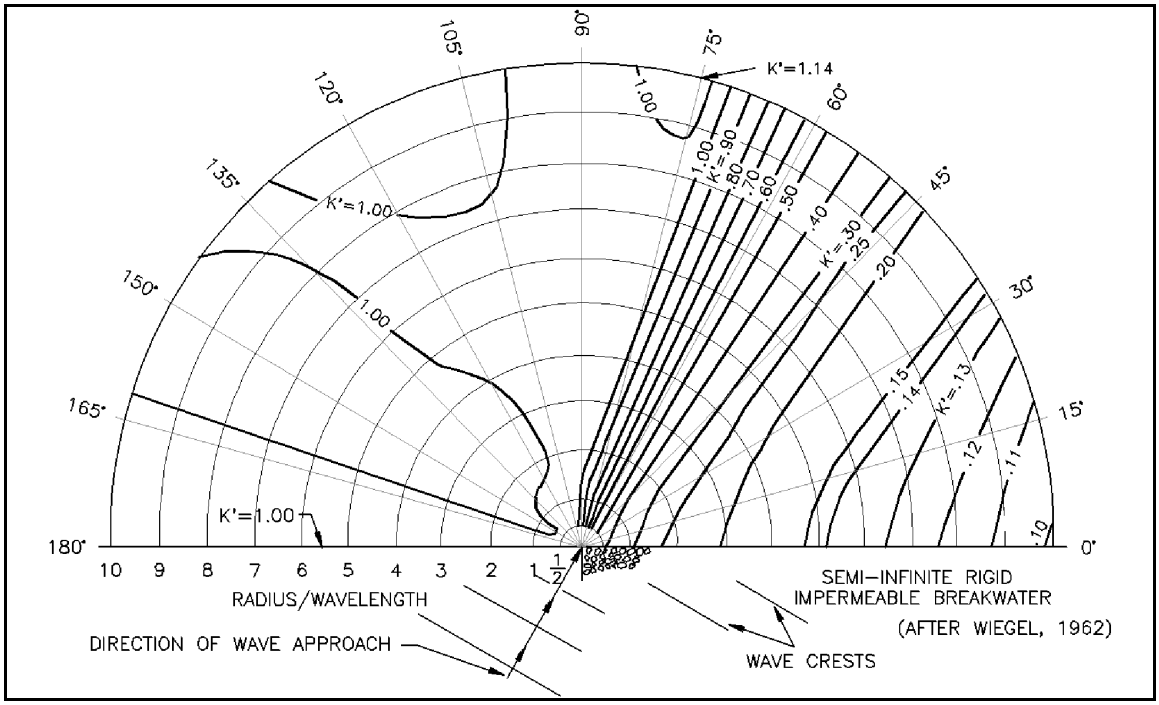

Figure II-7-3. Wave diffraction diagram - 60^0 wave angle

(f) Wave tank measurements of diffracted heights for waves passing a semi-infinite barrier were made by Putnam and Arthur (1948). They considered six approach directions for each of two incident wave periods. Their measurements generally confirm the diffraction theory. But, the diffraction theory assumes small-amplitude waves and Putnam and Arthur (1948) employed relatively small-amplitude waves in their experiments. For steeper waves, finite amplitude effects would cause the results to differ somewhat from the diffraction theory based on small-amplitude waves.

EXAMPLE PROBLEM II-7-1

FIND:

The wave height in the lee of the breakwater at a point specified by $\beta = 30$ deg and r = 100 m.

GIVEN:

A train of 6-sec-period 2-m-high waves is approaching a breakwater at an angle $\theta = 60$ deg. The water depth in the lee of the breakwater is 10 m.

SOLUTION:

From the linear wave theory for a period of 6 sec and a water depth of 10 m, the wave length can be calculated to be 48.3 m. Thus, $r/L = 100/48.3 = 2.07$. From Figure II-7-3 at $\beta = 30$ deg and r/L = 2.07, $K' = 0.28$. This yields a diffracted wave height = (0.28)2 = 0.56 m.

The diffracted wave would be propagating in the direction $\beta = 30$ deg and would have a continually diminishing wave height as indicated by Figure II-7-3. If the breakwater has a reflection coefficient that is less than one, the above result would still be reasonable, since the diffracted height of the reflected wave would be very small at the point of interest.

(2) Waves passing through a structure gap.

(a) When waves pass through a gap in a breakwater, diffraction occurs in the lee of the breakwater on both sides of the gap. As the waves propagate further into the harbor, the zone affected by diffraction grows toward the center line of the gap until the two diffraction zones interact (see Figure II-7-4). The wider the gap, the further into the harbor this interaction point occurs. For typical harbor conditions and gap widths greater than about five wavelengths, Johnson (1952) suggests that the diffraction patterns at each side of the gap opening will be independent of each other and Wiegel (1962) may be referenced for diffraction analysis. For smaller gap widths, an analysis employing the gap geometry must be used.

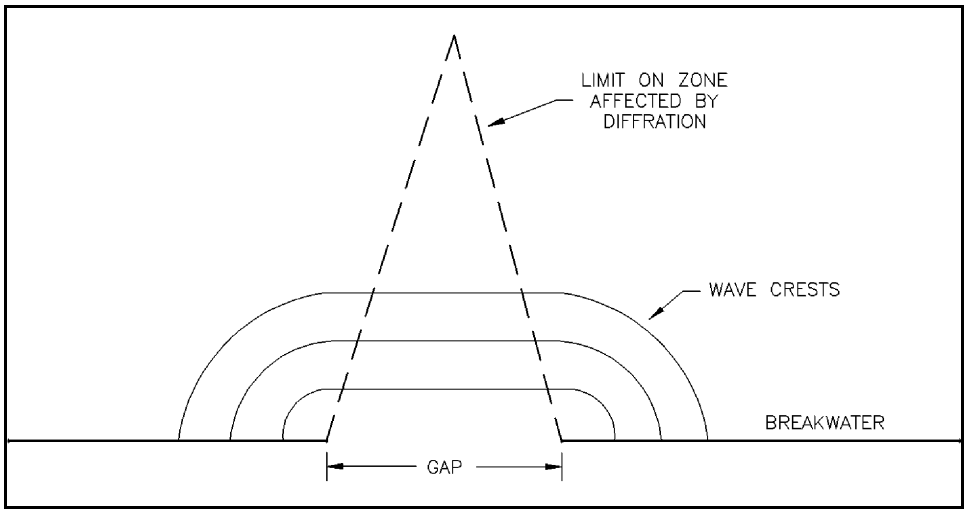

Figure II-7-4. Wave diffraction through a gap

(b) Penny and Price (1952) developed a solution for the diffraction of normally incident waves passing through a structure gap by superimposing the solutions for two mirror image semi-infinite breakwaters. Johnson (1952) employed their solution to develop diagrams that give diffraction coefficients for gap widths (B) that are between one half and five times the incident wavelength. The lateral coordinates (x,y) are again nondimensionalized by dividing by the wavelength. Figure II-7-5 is an example of one of the diagrams Johnson (1952) developed. Only one half of the pattern is shown; the other half would be a mirror image. The reader is referred to Johnson (1952) and the *Shore Protection Manual* (1984) when dealing with gap widths other than 0.5 wavelength.

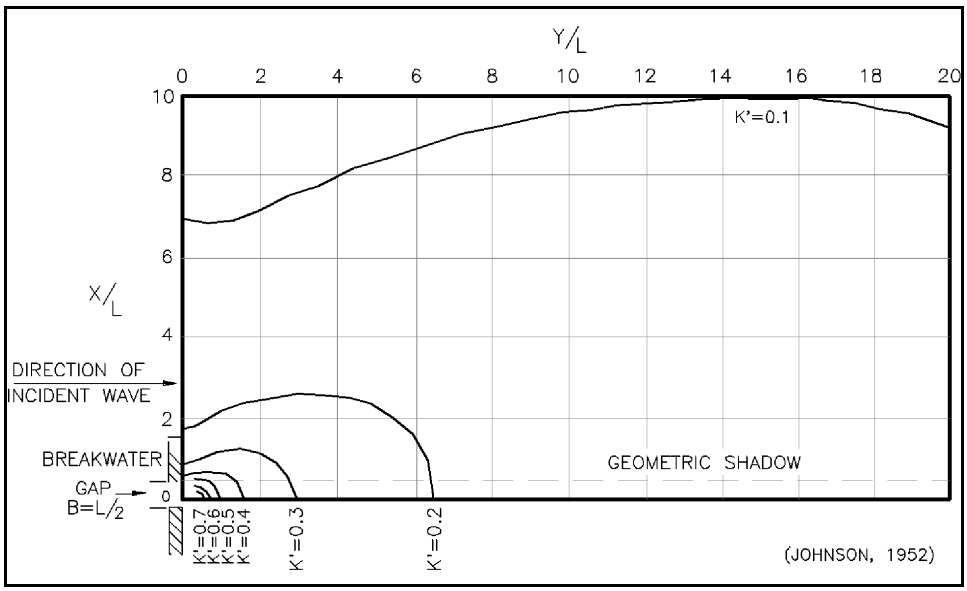

Figure II-7-5. Contours of equal diffraction coefficient gap width = 0.5 wavelength (B/L = 0.5)

(c) It may be necessary to know the wave crest orientation in the diffraction zone. Up to about six wavelengths beyond the gap, it is recommended (*Shore Protection Manual* 1984) that the wave crest position be approximated by two arcs that are centered on the two breakwater tips (as for a semi-infinite breakwater) and that the arcs be connected by a smooth curve that is approximately a circular arc centered on the midpoint of the gap. Beyond eight wavelengths, the crest position may be approximated by a single circular arc centered on the gap midpoint.

(d) The waves approaching a breakwater gap will usually not approach in a direction normal to the gap. Johnson (1952) found that the results presented above for normally incident waves can be used as an approximation for oblique waves by employing an imaginary equivalent gap having an orientation and width B' as defined in Figure II-7-6. Carr and Stelzriede (1952) employed a different analytical approach than that developed by Sommerfeld (1896) and also developed diffraction pattern solutions for barrier gaps that are small compared to the incident wavelength. Johnson (1952) used their approach to develop diffraction coefficient diagrams for a range of wave approach angles and a gap width equal to one wavelength. These are shown in Figures II-7-7 through II-7-12 for approach angles between 0 and 75 deg.

(e) Often, harbor entrance geometries will be different from the semi-infinite and gap geometries presented above. Still, approximate but useful results can be achieved by applying these solutions with some ingenuity in bracketing the encountered entrance geometry and interpolating results.

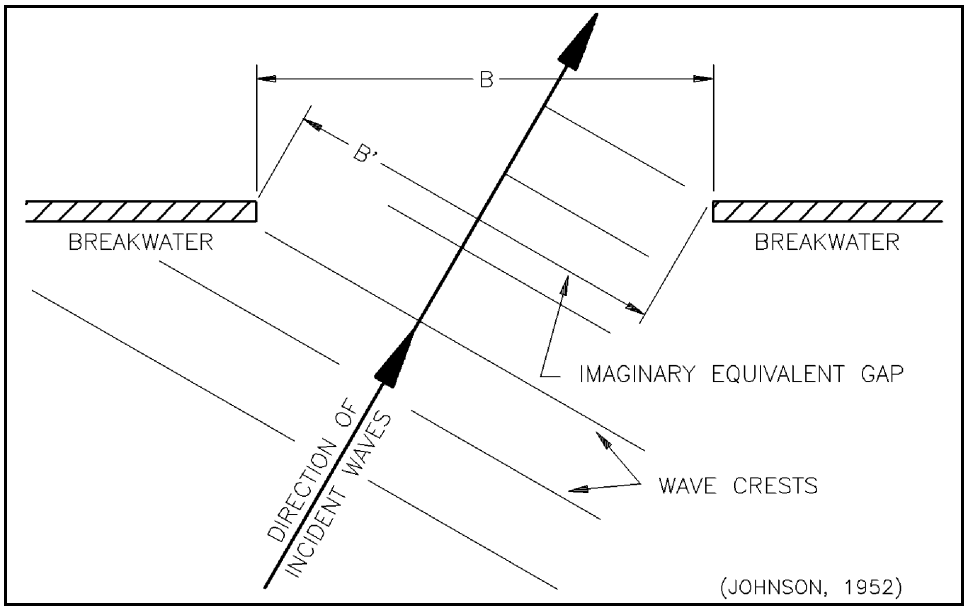

Figure II-7-6. Wave incidence oblique to breakwater gap

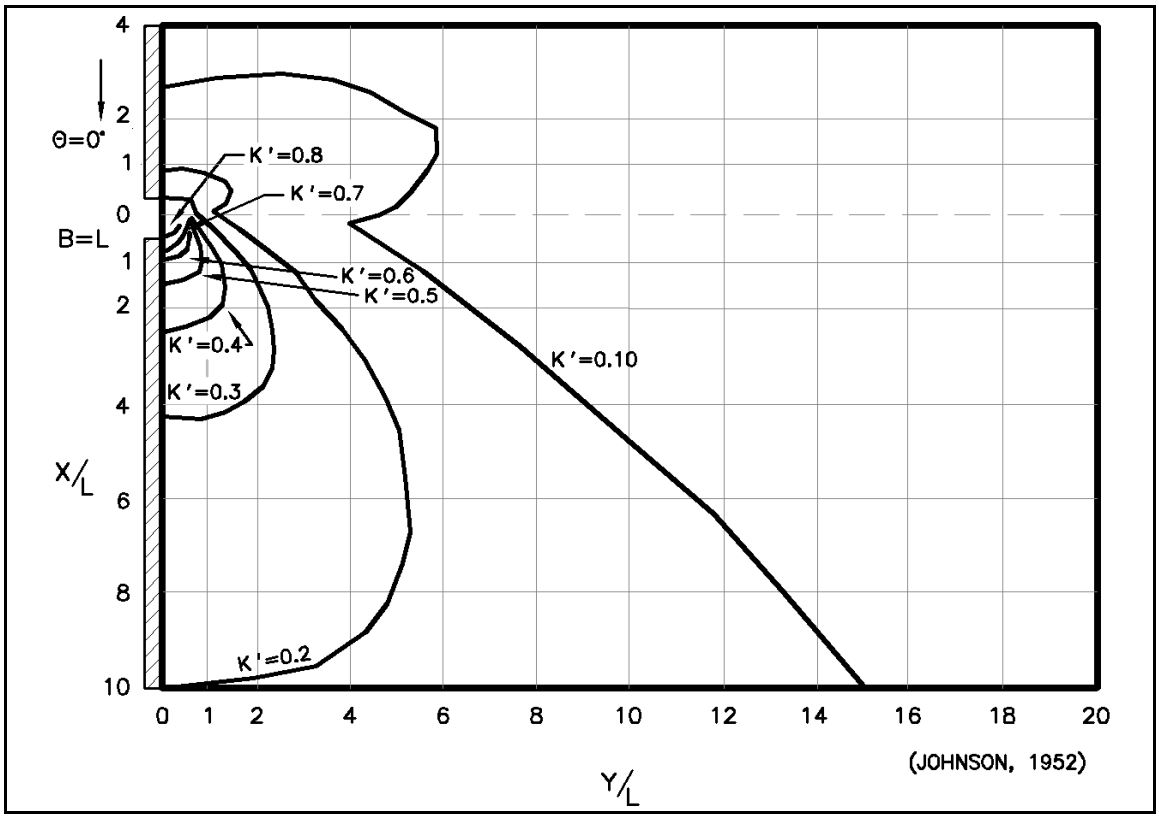

Figure II-7-7. Diffraction for a breakwater gap of one wavelength width where φ = 0 deg

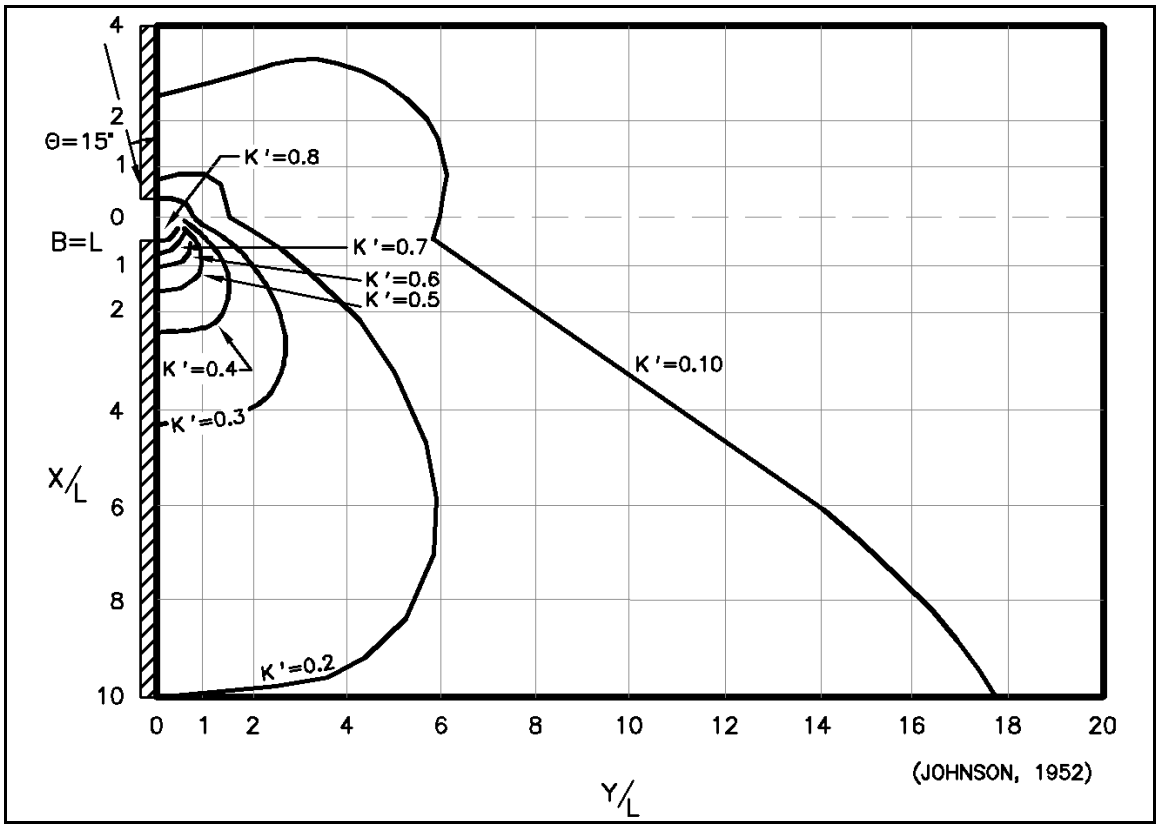

Figure II-7-8. Diffraction for a breakwater gap of one wavelength width where φ = 15 deg

(f) Bowers and Welsby (1982) conducted a physical model study of wave diffraction through a gap between two breakwaters whose axes are angled (rather than being collinear, i.e. 180 deg). Breakwater interior angles of 90 deg and 120 deg were employed. As would be expected, angling the breakwaters increased the heights behind the breakwater compared with the results for collinear breakwaters. But the increases were relatively small - up to 15 percent for 120-deg interior angles and up to 20 percent for 90-deg interior angles, when gap widths were in excess of half a wavelength.

(g) Memos (1976, 1980a, 1980b, 1980c) developed an approximate analytical solution for diffraction through a gap formed at the intersection of two breakwaters having axes that are not collinear but intersect at an angle. The point of intersection of the breakwater axes coincides with the tip of one of the breakwaters. Memos' solution can be developed for various angles of wave approach.

d. Irregular wave diffraction.

(1) The preceding discussion of wave diffraction was concerned with monochromatic waves. The effects of wave diffraction on an individual wave depend on the incident wave frequency and direction. Thus, each component of a directional wave spectrum will be affected differently by wave diffraction and have a different K' value at a particular point in the lee of a breakwater.

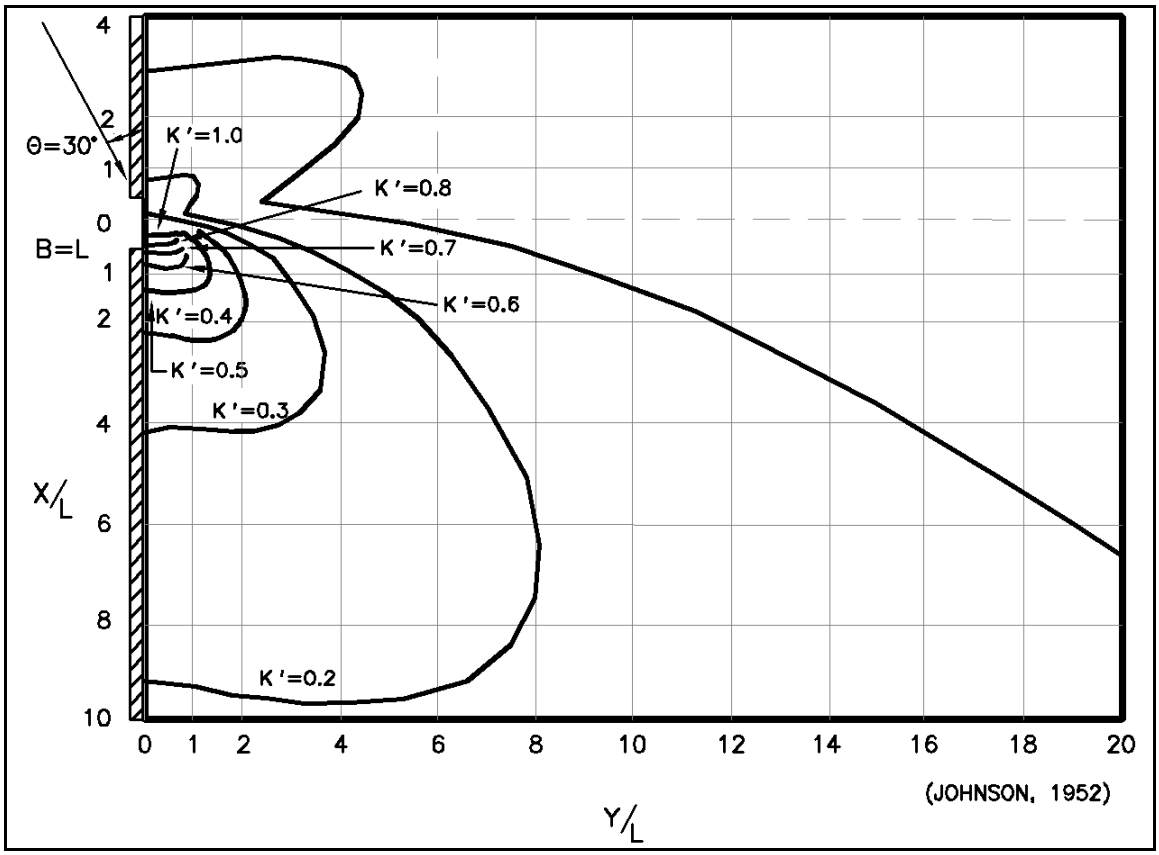

Figure II-7-9. Diffraction for a breakwater gap of one wavelength width where φ = 30 deg

(2) To evaluate the effect of diffraction on a directional wave spectrum, Goda, Takayama, and Suzuki (1978) calculated diffraction coefficients for a semi-infinite breakwater and a breakwater gap by breaking the spectrum into number of frequency (10) and direction (20 to 36) components and combining the result at points in the breakwater lee. This produced an effective diffraction coefficient defined by

$$K_e' = \left[\frac{1}{M_o} \int_0^{\infty} \int_{\theta\ \min}^{\theta\ \max} S(f,\theta)\ (K')^2\ d\ \theta\ df \right]^{\frac{1}{2}} \qquad \text{(II-7-1)}$$

where K' is the diffraction coefficient for each frequency/direction component when acting as a monochromatic wave, M_0 is the zero moment of the spectrum, df and dθ are the frequency and direction ranges represented by each component of the spectrum, θ_{max} and θ_{min} are the limits of the spectral wave component directions, and $S(f,\theta)$ is the spectral energy density for the individual components. The spectral frequency distribution they employed was similar to most typical storm spectra such as the JONSWAP spectrum. The directional spread of the spectrum was characterized by a directional concentration parameter S_{max}, which equals 10 for widely spread wind waves and 75 for swell with a long decay distance, so the directional spread is quite limited.

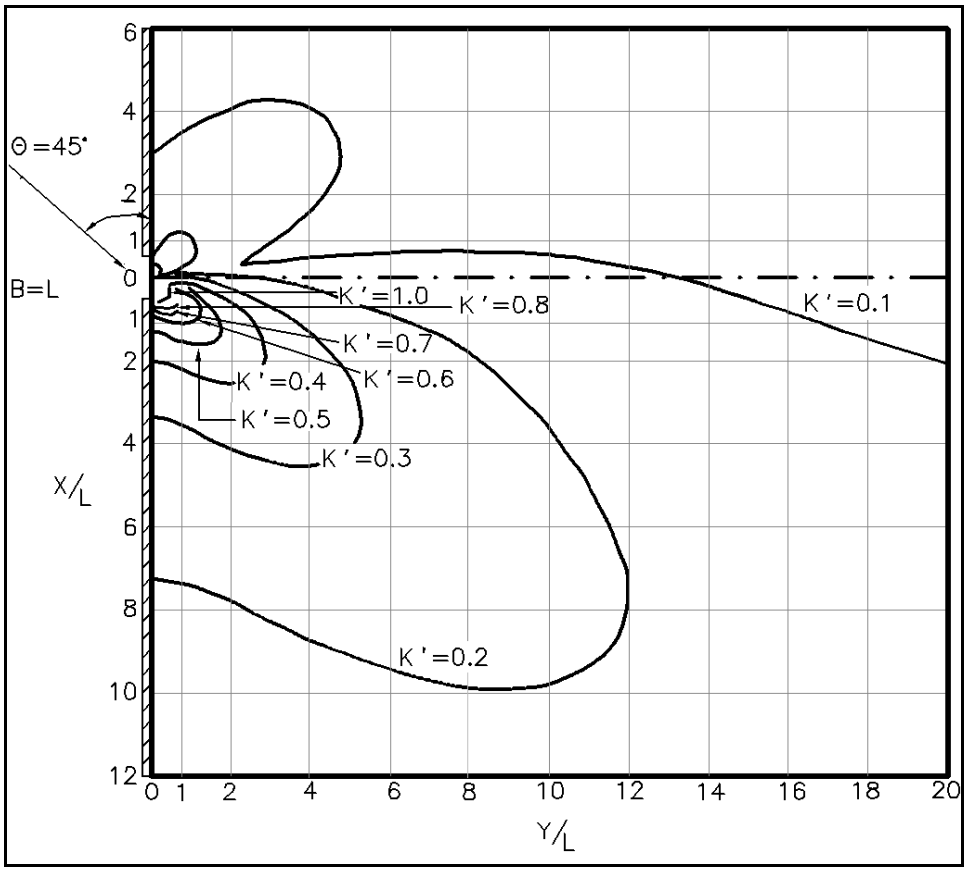

Figure II-7-10. Diffraction for a breakwater gap of one wavelength width where φ = 45 deg

(3) The results for waves approaching perpendicular to a semi-infinite breakwater are shown in Figure II-7-13 where the solid lines define values of K'_e and the dashed lines are the ratio of peak spectral period for the diffracted to incident waves. The results for waves approaching normal to a breakwater gap are shown in Figures II-7-14 to II-7-17, where the ratio of gap width to incident wavelength varies from 1 to 8. Note that these diagrams are normalized by dividing by both the gap width and the wavelength, so two different horizontal scales are given for each case. Also, the left-hand side gives the peak period ratio and the right-hand side gives values of K'_e.

(4) The spectral diffraction diagrams for the semi-infinite breakwater show a small change in the peak period ratio as the waves extend into the breakwater lee. (For monochromatic waves the wave period would not change.) The same holds for the breakwater gap. For the semi-infinite breakwater the values of K'_e are generally higher than the equivalent values of K' for monochromatic waves. For a breakwater gap, the spatial variation of K'_e values is smoothed out by the directional spread of the incident waves. That is, there is less variation in K'_e values for the spectral case than in K' for the monochromatic case. For waves approaching a breakwater gap at some oblique angle, the imaginary equivalent gap approach depicted in Figure II-7-6 can be used.

(5) Thus, if the one-dimensional or directional spectrum for the design waves is known at a harbor entrance, Equation II-7-1 can be used with the monochromatic wave diffraction diagrams to more effectively evaluate wave diffraction in the harbor. The spectrum can be broken into a number of direction and/or frequency components, each component can be analyzed as a diffracting monochromatic wave, and the results can be recombined using Equation II-7-1.

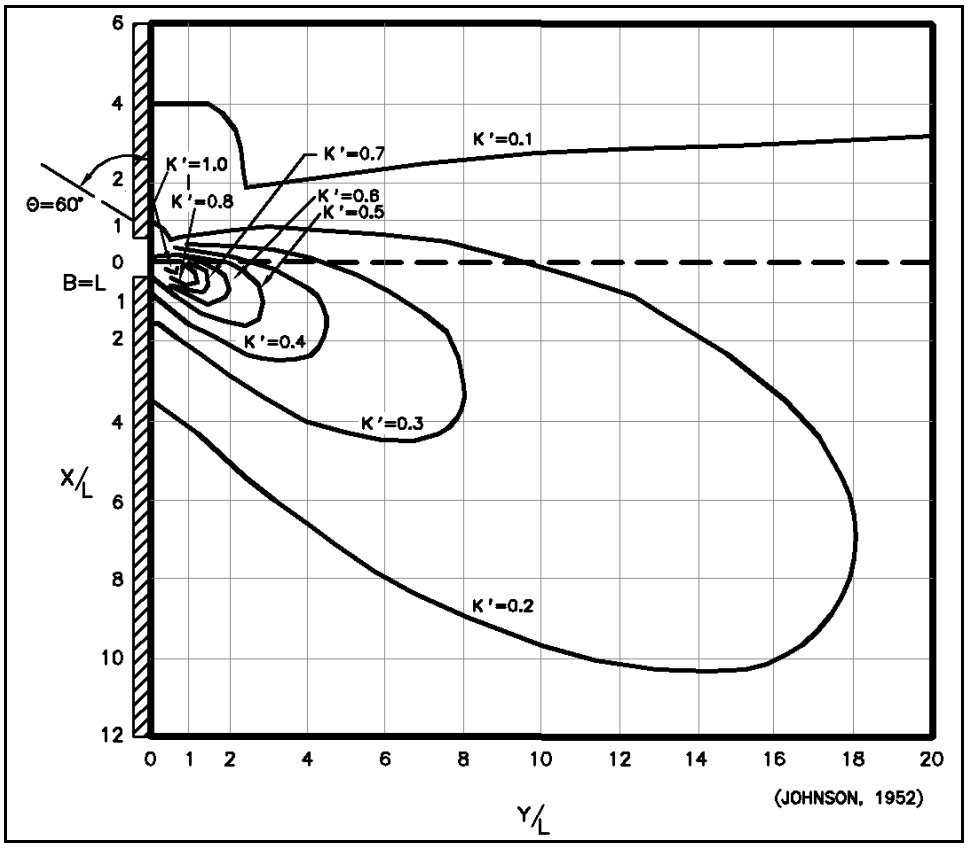

Figure II-7-11. Diffraction for a breakwater gap of one wavelength width where φ = 60 deg

e. Combined refraction-diffraction in harbors.

(1) In most harbors, the depth is relatively constant so the diffraction analyses discussed above are adequate to define the resulting wave conditions. However, if the depth changes significantly, then wave amplitudes will change because of shoaling effects. If the harbor bottom contours are not essentially parallel to the diffracting wave crests, then wave amplitudes and crest orientations will be affected by refraction.

(2) Where depth changes in a harbor are sufficient for combined refraction and diffraction effects to be significant, the resulting wave height and direction changes can be investigated by either a numerical or a physical model study. For examples of numerical model studies of combined refraction-diffraction in the lee of a structure, see Liu and Lozano (1979), Lozano and Liu (1980), and Liu (1982). Physical models that investigate the combined effects of refraction and diffraction are routinely conducted (see Hudson et al. 1979). The one major limitation on these models for wind wave conditions is that the model cannot have a distorted scale (i.e., horizontal and vertical scale ratios must be the same). Sometimes, lateral space limitations or the need to maintain an adequate model depth to avoid viscous and surface tension scale effects make a distorted scale model desirable. But such a model cannot effectively investigate combined refraction-diffraction problems.

(3) In many cases, the depth near the entrance to a harbor is relatively constant with the significant depth changes occurring further from the entrance (in the vicinity of the shoreline). Then an approximate (but often adequate) analysis can be carried out using the techniques discussed herein. The diffraction analysis would be carried out from near the harbor entrance to the point inside the harbor where significant

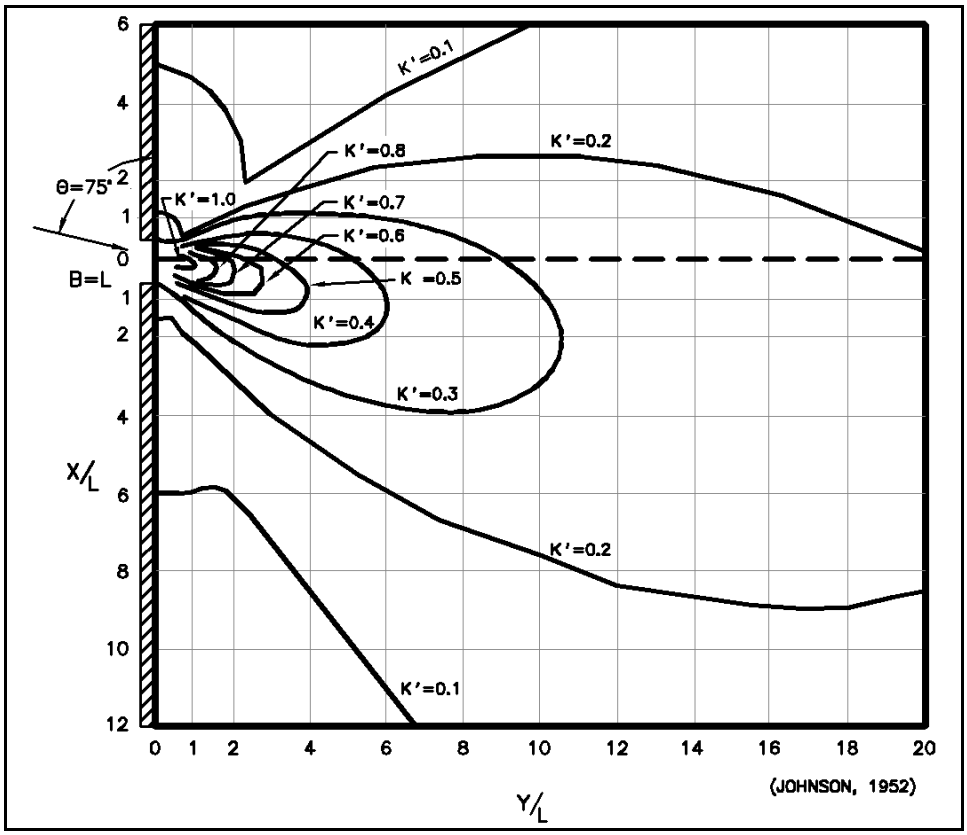

Figure II-7-12. Diffraction for a breakwater gap of one wavelength width where φ = 75 deg

depth changes commence. Hopefully, this will be a distance of at least three or four wavelengths from the entrance. This diffraction analysis will define the wave heights and crest orientation at the point where significant shoaling-refraction effects commence. From this point landward, a refraction-shoaling analysis using the procedures described in Part II-3 can be used to carry the wave to the point of breaking or interaction with a land boundary.

f. Combined diffraction - reflection in harbors.

(1) A computer program for dealing with combined diffraction and reflection by a vertical wedge has been developed by Seelig (1979, 1980) and is available in the Automated Coastal Engineering System (ACES) (Leenknecht et al. 1992). This package estimates wave height modifications due to combined diffraction and reflection caused by a structure. It has the ability to simulate a single straight, semi-infinite breakwater, corners of docks, and rocky headlands. Assumptions include monochromatic, linear waves, and constant water depth.

(2) The user has the ability to vary the wedge angle from 0 to 180 deg, where 0 deg would represent the case of a single straight, semi-infinite breakwater and 90 deg, the corner of a dock.

(3) The required input includes incident wave height, wave period, water depth, wave angle, wedge angle, and X and Y coordinates (location of desired calculation). The range of X and Y should be limited to plus or minus 10 wavelengths.

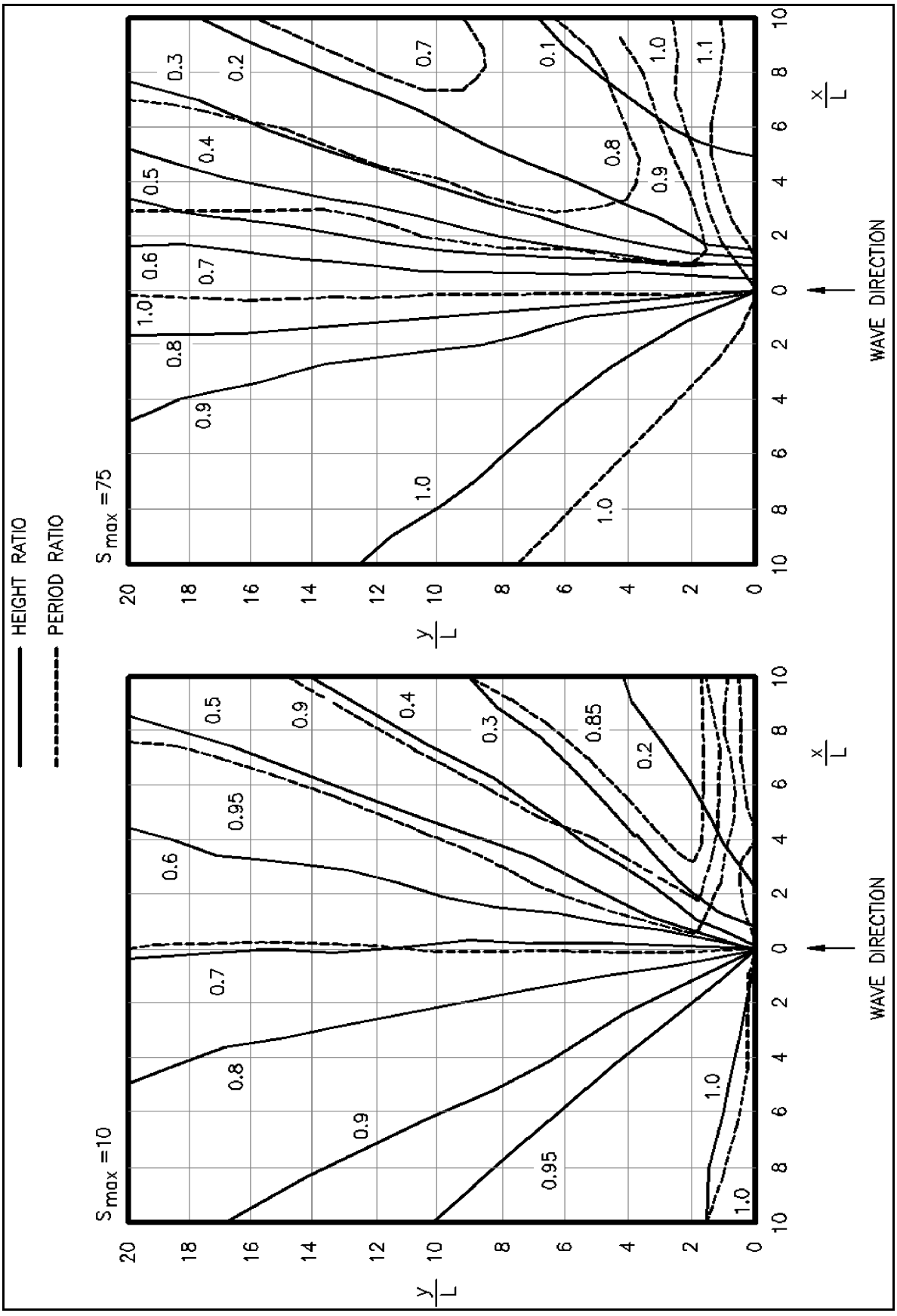

Figure II-7-13. Diffraction diagram of a semi-infinite breakwater for directional random waves of normal incidence (Goda 2000)

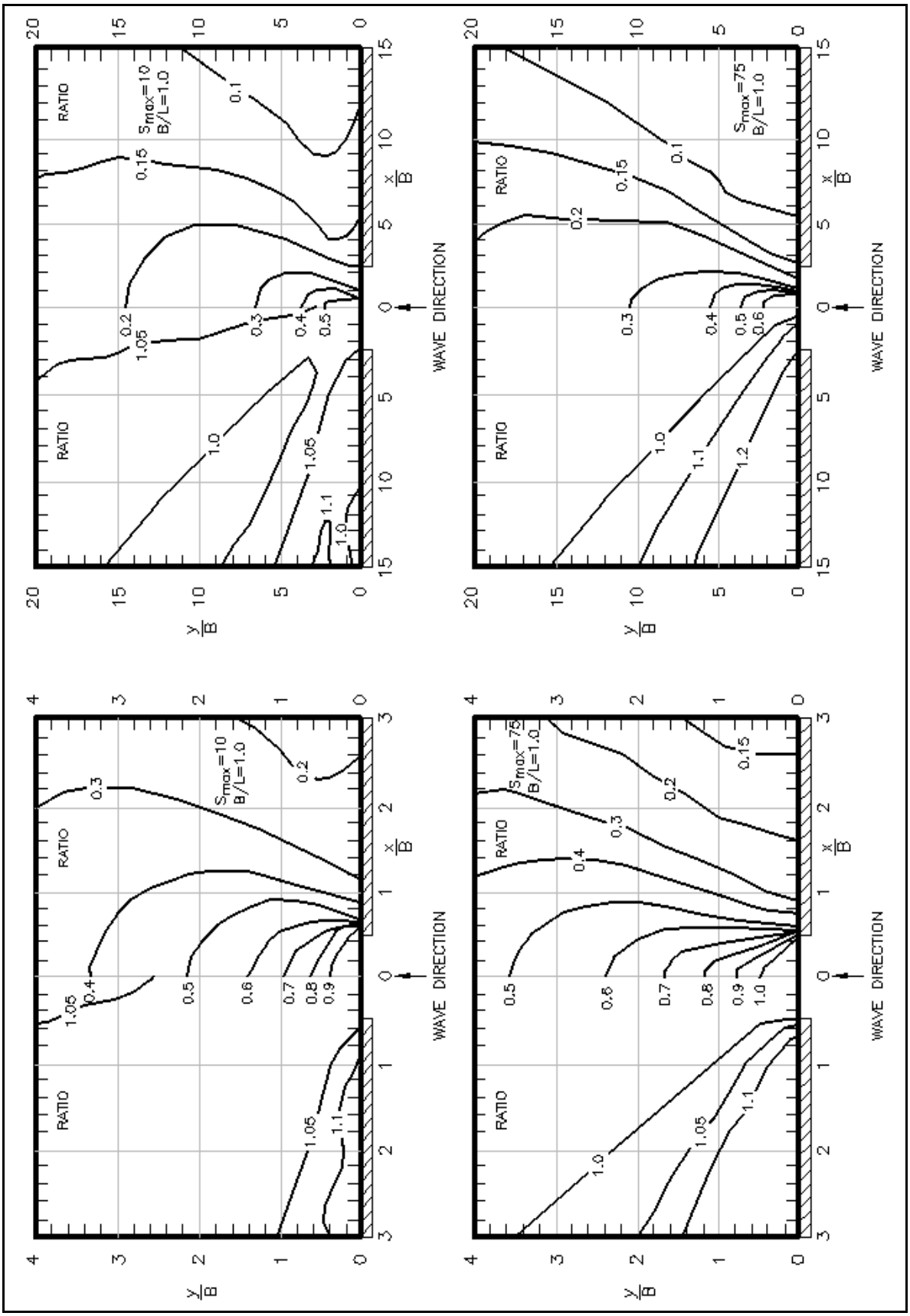

Figure II-7-14. Diffraction diagrams of a breakwater gap with *B/L* = 1.0 for directional random waves of normal incidence (Goda 2000)

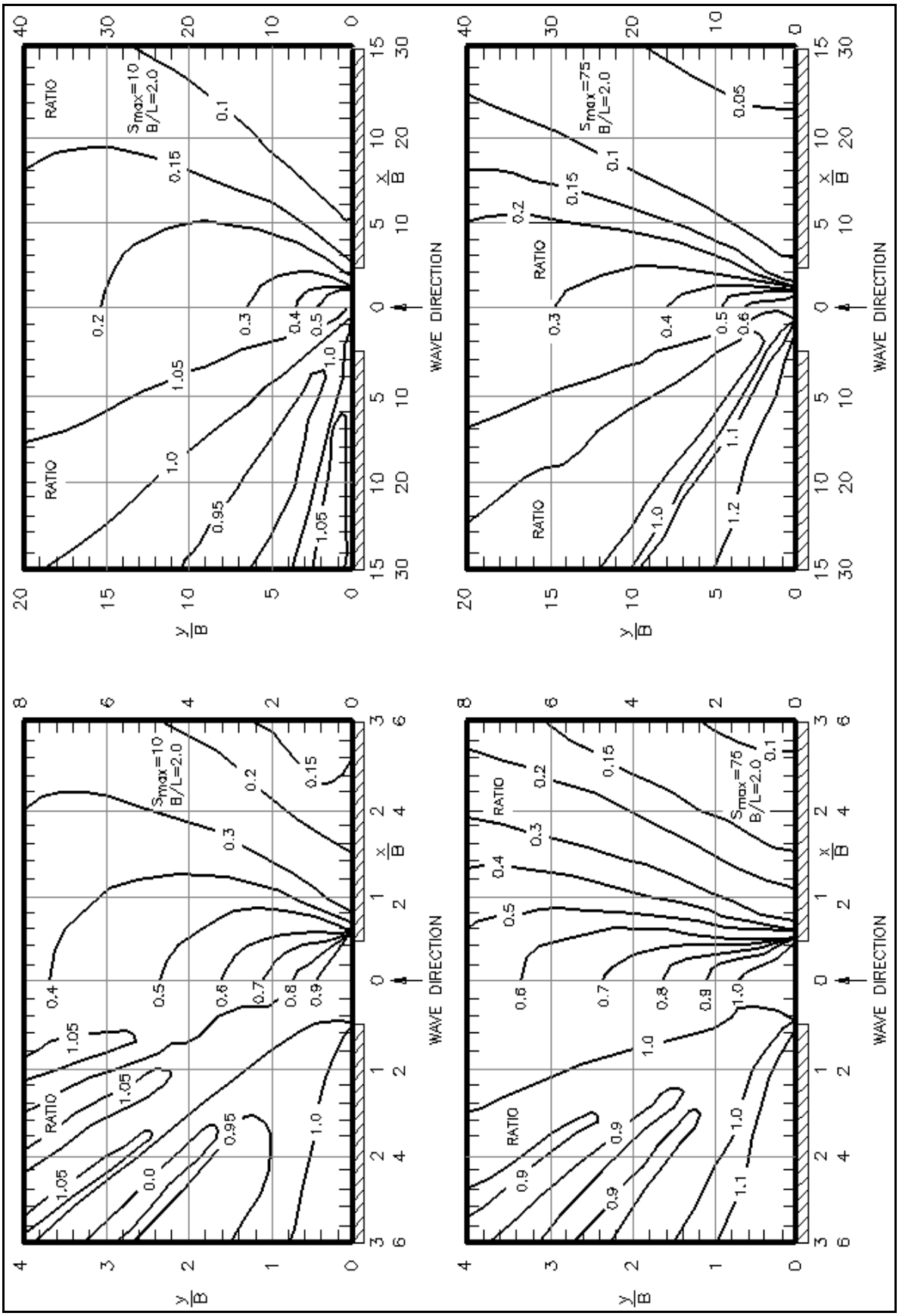

Figure II-7-15. Diffraction diagrams of a breakwater gap with *B/L* = 2.0 for directional random waves of normal incidence (Goda 2000)

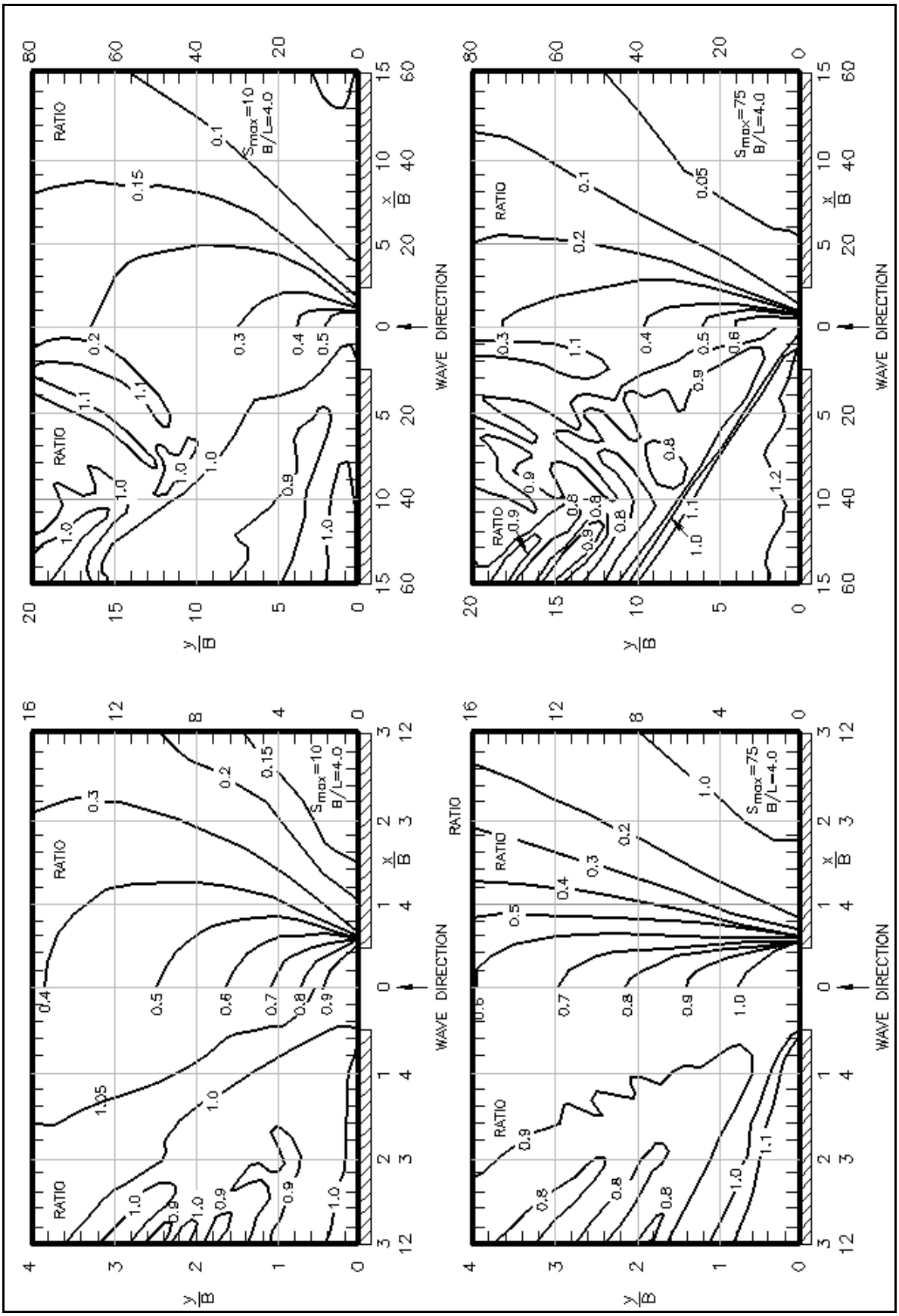

Figure II-7-16. Diffraction diagrams of a breakwater gap with *B/L* = 4.0 for directional random waves of normal incidence (Goda 2000)

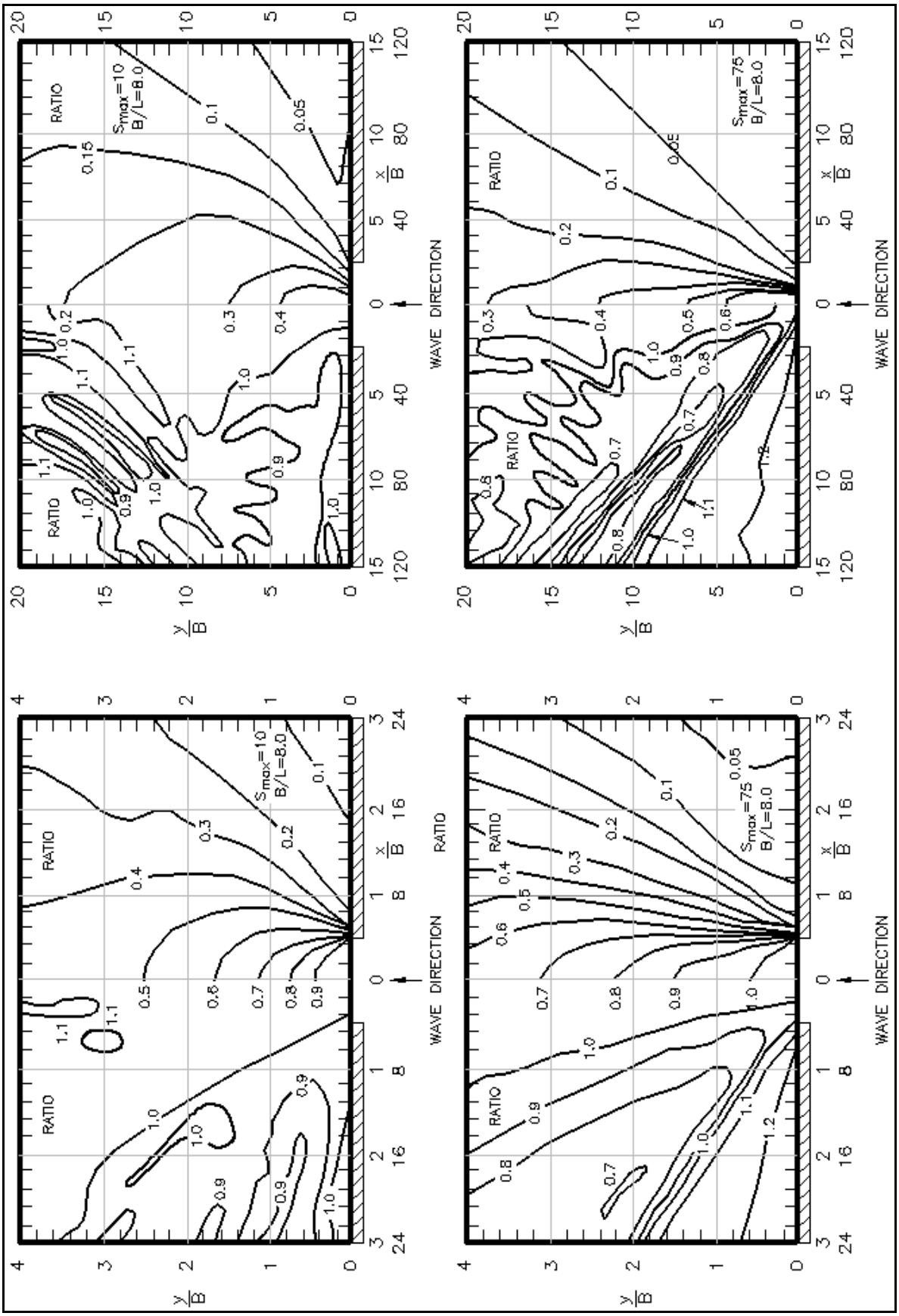

Figure II-7-17. Diffraction diagrams of a breakwater gap with *B/L* = 8.0 for directional random waves of normal incidence (Goda 2000)

(4) The wavelength, ratio of calculated wave height to incident wave height, wave phase, and modified wave height are given as output data. For further information on the ACES system, the reader is referred to Leenknecht et al. (1992).

II-7-3. Wave Transmission

a. Definition of transmission.

(1) When waves interact with a structure, a portion of their energy will be dissipated, a portion will be reflected and, depending on the geometry of the structure, a portion of the energy may be transmitted past the structure. If the crest of the structure is submerged, the wave will simply transmit over the structure. However, if the crest of the structure is above the waterline, the wave may generate a flow of water over the structure which, in turn, regenerates waves in the lee of the structure. Also, if the structure is sufficiently permeable, wave energy may transmit through the structure. When designing structures to protect the interior of a harbor from wave attack, as little wave transmission as possible should be allowed, while optimizing the cost versus performance of the structure.

(2) Transmitted wave height will be less than incident wave height, and wave period will usually not be identical for transmitted and incident waves. Laboratory experiments conducted with monochromatic waves typically show that the transmitted wave has much of its energy at the same frequency as the incident wave, but a portion of the transmitted energy has shifted to the higher harmonic frequencies of the incident wave. For a given incident wave spectrum, there would be a commensurate shift in the transmitted wave spectrum to higher frequencies.

(3) The degree of wave transmission that occurs is commonly defined by a wave transmission coefficient $C_t = H_t/H_i$ where H_t and H_i are the transmitted and incident wave heights, respectively. When employing irregular waves, the transmission coefficient might be defined as the ratio of the transmitted and incident significant wave heights or some other indication of the incident and transmitted wave energy levels.

(4) Most quantitative information on wave transmission past various structure types has necessarily been developed from laboratory wave flume studies. Historically, most of the early studies employed monochromatic waves; but, during the past two decades there has been a significant growth in information based on studies with irregular waves.

b. Transmission over/through structures.

(1) Rubble-mound structures-subaerial.

(a) Figure II-7-18 is a schematic cross section of a typical rubble-mound structure. The freeboard F is equal to the structure crest elevation h minus the water depth at the toe of the structure d_s (i.e., $F = h - d_s$). Also shown is the wave runup above the mean water level R that would occur if the structure crest elevation was sufficient to support the entire runup. When $F < R$, wave overtopping and transmission will occur. The parameter F/R is a strong indicator of the amount of wave transmission that will occur. Procedures for determining wave runup are presented elsewhere in the CEM.

(b) A number of laboratory studies of wave transmission by overtopping of subaerial structures have been conducted (see *Shore Protection Manual* (1984)). The most recent and comprehensive of these studies was conducted by Seelig (1980), who also studied submerged breakwaters.

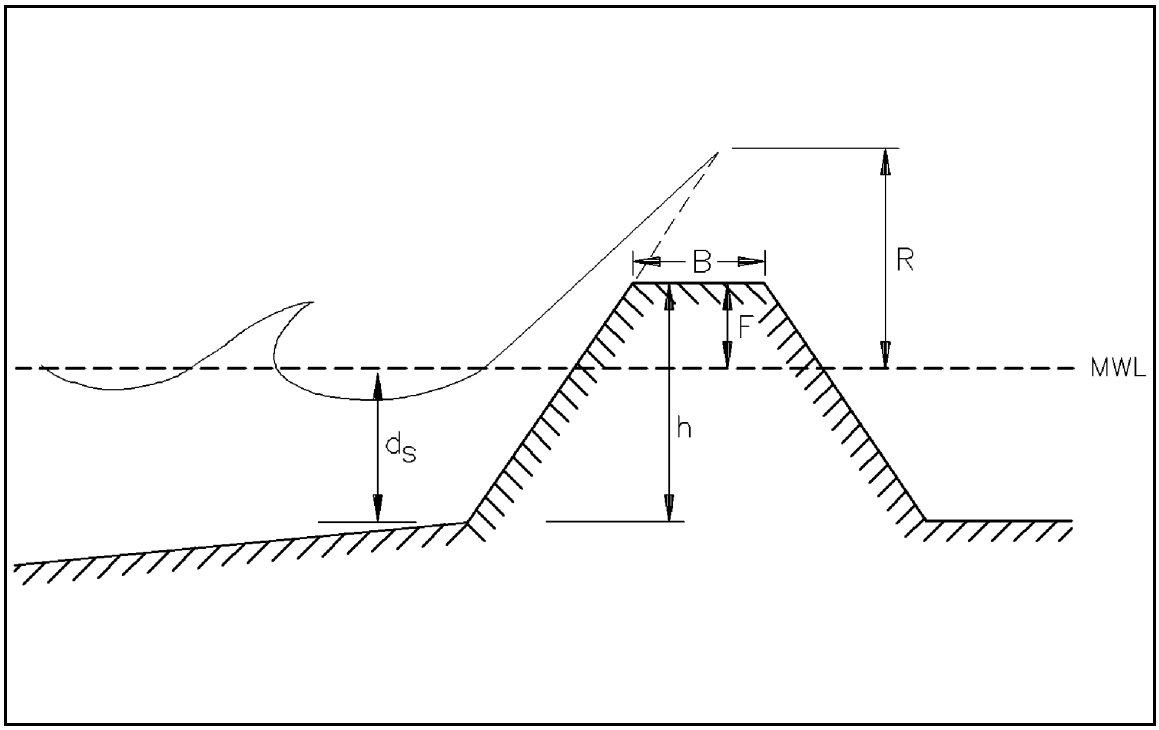

Figure II-7-18. Schematic breakwater profile and definition of terms

(c) Seelig presented a simple formula for estimating the wave transmission coefficient for subaerial stone mound breakwaters, which is valid for both monochromatic and irregular waves:

$$C_t = C\left(1 - \frac{F}{R}\right) \tag{II-7-2}$$

(d) The coefficient C is given by

$$C = 0.51 - \frac{0.11B}{h} \tag{II-7-3}$$

where B is the structure crest width and h is the crest elevation above the bottom (see Figure II-7-18). It is recommended that Equation II-7-2 be applied to the relative depth (d_s/gT^2) range of 0.03 to 0.006 and Equation II-7-3 to the range of B/h between 0 and 3.2, because these are the ranges of experimental data employed to develop the equations.

(e) The report by Seelig (1980) contains laboratory results for 19 different breakwater cross-section geometries. Specific results for one or more of these geometries may closely relate to the prototype structure being analyzed. For irregular waves, the wave transmission coefficients were defined in terms of the incident and transmitted spectral energies.

(2) Rubble-mound structures-submerged.

(a) Rubble-mound structures having their crest at or below the mean water level have seen increasing use recently. Often, they simply consist of a homogeneous wide-graded mass of stone. A functional

advantage for these lower-cost structures is that they may have a relatively high transmission coefficient for everyday lower waves, but as the height of the incident waves increases, the transmission coefficient will generally decrease. For harbor installations, they have been used in tandem with a conventional subareal breakwater placed in their lee - the combined cost of the two structures being less than a single structure with the same operational criteria (Cox and Clark 1992). A number of laboratory experiments on wave transmission past submerged rubble-mound structures have been conducted. Results are summarized in Seelig (1980) and Van der Meer and Angremond (1992).

(b) Van der Meer and Angremond (1992) summarized the available data plus some of their own data to present a comprehensive procedure for predicting wave transmission for low-crested breakwaters. For irregular waves they defined the transmission coefficient as the ratio of incident and transmitted significant wave heights. They correlated C_t with F/H_i where F would have positive values for low subaerial breakwaters and negative values for breakwaters with a submerged crest. Correlations with parameters that also included the incident wave period did not improve results. Figure II-7-19 gives C_t versus F/H_i.

(c) Van der Meer and Angremond (1992) were able to improve the correlations based on experimental data by introducing the median diameter D_{50} of the armor stone used to build the structure. (There is a relationship between D_{50} and the design wave height for a stable structure.) They then correlated C_t with F/D_{50} and secondary factors H_s/gT_p^2, H_i/D_{50}, and B/D_{50}. These relationships are presented in the form of somewhat complex formulas.

(3) Permeable rubble-mound structures.

(a) Wave energy may transmit through a rubble-mound structure, particularly if it is constructed solely of a homogeneous mass of large diameter stone. If the structure contains a number of stone layers including a core of fine stones, the wave transmission will be much less. Also, wave energy transmission through a stone mound structure would be significant for long-period, low waves, but much less for shorter-period waves (e.g. the tide would only be slightly reduced by a rubble-mound structure, but steep, wind-generated waves would have negligible transmission through the structure).

EXAMPLE PROBLEM II-7-2

FIND:

The transmission coefficients and the transmitted wave heights for incident wave heights of 0.5, 1.0, 2.0 and 4.0 m.

GIVEN:

A submerged offshore breakwater situated where the bottom is 4.0 m below the design still-water level. The structure crest elevation is 3.0 m above the bottom.

SOLUTION:

The breakwater freeboard F is 3.0 - 4.0 = -1.0 m. Employing Figure II-7-19 we have:

$H_{i(m)}$	F/H_i	C_t	$H_{t(M)}$
0.5	-2.0	0.82	0.41
1.0	-1.0	0.74	0.74
2.0	-0.5	0.60	1.20
4.0	-0.25	0.52	2.10

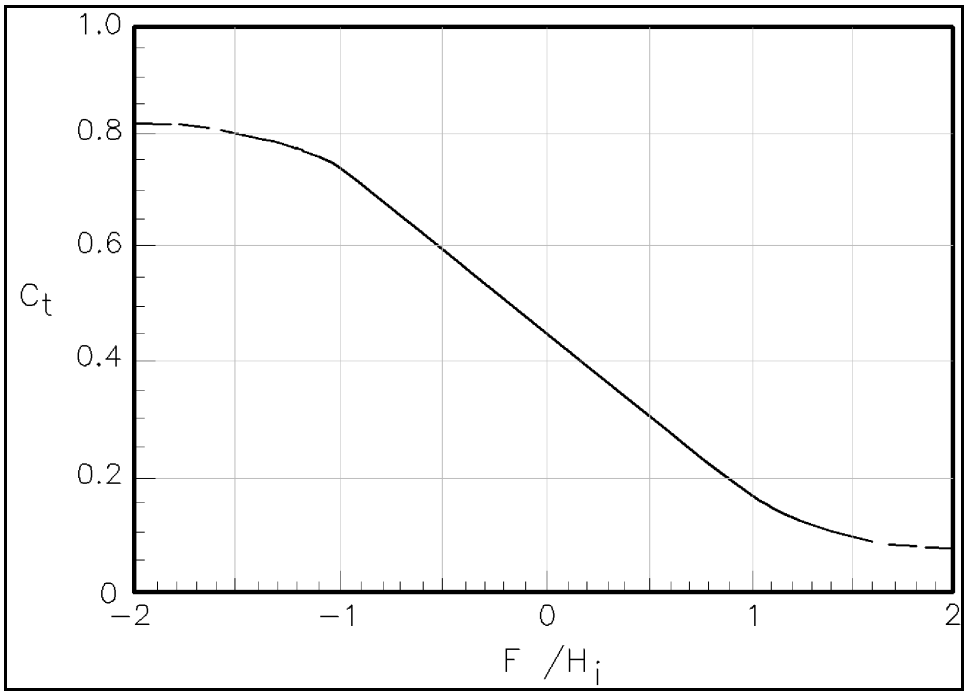

Figure II-7-19. Wave transmission for a low-crested breakwater (modified from Van der Meer and Angremond (1992))

(b) When a porous rubble-mound structure suffers wave transmission caused by wave overtopping and by wave propagation through the structure, the resulting combined transmission coefficient would be

$$C_t = \sqrt{C_{tt}^2 + C_{t0}^2} \tag{II-7-4}$$

where C_{tt} is the coefficient for wave transmission through the structure and C_{t0} is the coefficient for wave transmission by flow over the structure.

(c) Potential scale effects make it difficult to conduct scaled laboratory experiments to measure wave transmission through rubble-mound structures. (Wave motion requires Froude similitude, while flow through porous media requires Reynolds similitude, but the two are incompatible.) Consequently, the best procedure for determining C_{tt} for a rubble-mound structure is a numerical procedure developed by Madsen and White (1976). A computer program for applying this procedure has been developed by Seelig (1979,1980) and is available in the ACES system (Leenknecht et al. 1992).

(d) The procedure developed by Madsen and White (1976) first calculates the amount of wave dissipation caused by wave runup/rundown on the seaward face of the structure. (It is assumed that the wave does not break - a good assumption for longer waves.) Wave reflection from the structure is also determined. The remaining energy propagates into the structure and is partially dissipated by turbulent action. The procedure then determines this rate of turbulent energy dissipation assuming a rectangular homogeneous breakwater cross section that is hydraulically equivalent to the actual layered breakwater. This leads to the transmitted wave height and C_{tt}. Application of this procedure requires a knowledge of the incident wave height and period, the water depth, the breakwater layer geometry, and the stone sizes and porosities for each layer. Seelig (1980) found that this procedure could be applied to irregular waves by using the mean wave height and spectral peak period of the incident waves in the calculation.

EXAMPLE PROBLEM II-7-3

FIND:

The transmission coefficient for incident waves having periods of 2 and 5 sec.

GIVEN:

The catamaran breakwater whose performance is depicted in Figure II-7-21.

SOLUTION:

For a water depth of 7.6 m, using the linear wave theory, wavelengths would be calculated to be 6.24 m (for T = 2 sec) and 34.4 m (for T = 5 sec). For a width W of 6.4 m, this yields W/L = 1.03 and 0.186, respectively. From Figure II-7-21, this yields C_t = 0.2 (extrapolating) for the 2-sec wave and C_t = 0.8 for the 5-sec wave. Thus, this catamaran is quite effective for the 2-sec wave but quite ineffective for the 5-sec wave.

(4) Floating breakwaters.

(a) Moored floating breakwaters have some distinct advantages for harbor installations. They are more adaptable to the water level changes that occur at harbors that are built on reservoirs and in coastal areas having a large tidal range. They are usually more economical than fixed breakwaters for deep-water sites, and they interfere less with water circulation and fish migration. But they also have some significant limitations. Since they are articulating structures, they are prone to damage at connecting points between individual breakwater units and between these units and mooring lines. And, their performance is very dependent on the period of the incident waves. This last factor will establish relatively severe limits on where floating breakwaters can effectively be deployed.

(b) Several different types of floating breakwaters have been proposed. Hales (1981) presents a survey of these various types and their performance. Most of the floating breakwaters in use are of three generic types - prism, catamaran, and scrap tire assembly (see Figure II-7-20). Figure II-7-21 plots the wave transmission coefficients for a typical representative of each of these three types. The transmission coefficient is plotted versus the breakwater's characteristic dimension in the direction of wave propagation W divided by the incident wave length L at the breakwater. The data plotted in Figure II-7-21 are all derived from laboratory experiments. The prism results are for a concrete box having a 4.88-m width (W), a draft of 1.07 m, and a water depth of 7.6 m (Hales 1981). The catamaran (Hales 1981) has two pontoons that are 1.07 m wide with a draft of 1.42 m and a total width (W) of 6.4 m. The water depth was 7.6 m. The tire assembly (Giles and Sorensen 1979) had a width of 12.8 m (W), a nominal draft of one tire diameter, and was tested in water 3.96 m deep. The three breakwaters were all moored fore and aft; other mooring arrangements would somewhat alter the transmission coefficient.

(c) Example Problem II-7-3 demonstrates a major limitation of floating breakwaters. For typical breakwater sizes (i.e., W equals 5 to 10 m) the incident wave period must not exceed 2-3 sec for the breakwater to be very effective. Thus, for typical design wind speeds, the fetch generating the waves to which the structure is exposed cannot be very large. Sorensen (1990) conducted an analysis to determine general wind speed, fetch, and duration guidelines for the three floating breakwaters from Figure II-7-20. He assumed an allowable transmitted wave height of 2 ft (0.61 m). For example, for a wind speed of 60 mph (26.8 m/sec) having a duration of 20-30 min, the fetch must not exceed 2-3 miles (3.2-4.8 km) if the transmitted wave height is to be less than 2 ft.

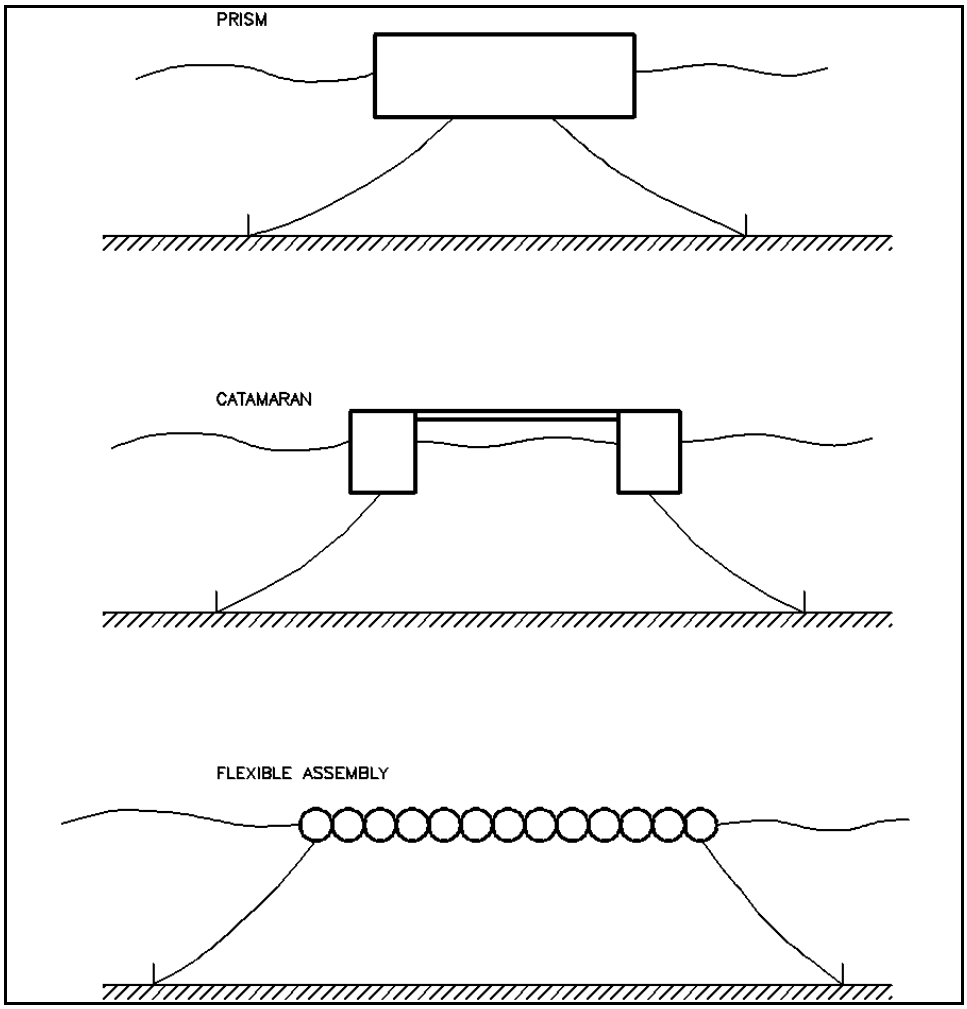

Figure II-7-20. Common types of floating breakwaters

(d) The wave-induced loading on the floating breakwater's mooring/anchor system is also an important design concern. Hales (1981) and Harms et al. (1982) present mooring load data for various types of floating breakwaters. The peak mooring load that develops for a given breakwater geometry and mooring arrangement depends primarily on the incident wave height and increases significantly as the wave height increases; the wave period or length is only of secondary importance in determining the mooring load. If the mooring load cannot be adequately estimated from published information on similar breakwaters, physical model tests may be required to determine these loads for the anticipated design wave conditions.

(5) Wave barriers.

(a) Vertical thin semirigid barriers are used as breakwaters at some harbors, particularly where wave loading is relatively small and wave reflection would not be a problem. For some small-craft harbor installations, the barrier is open at the bottom, which allows water to circulate in and out of the harbor and reduces structure costs (see Gilman and Nottingham (1992) and Lott and Hurtienne (1992). If the incident wave period is relatively short (d/L relatively large), wave action is focused near the surface and wave transmission would be relatively small.

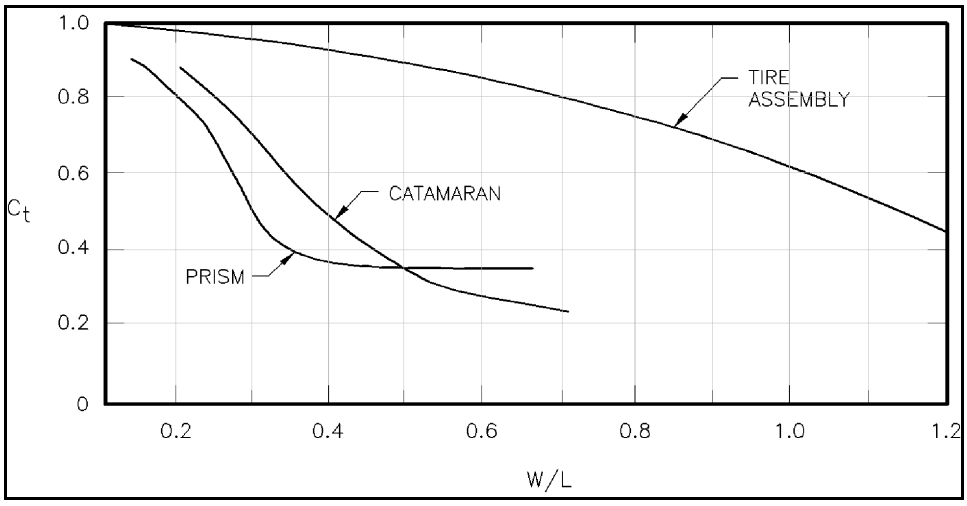

Figure II-7-21. Wave transmission coefficient for selected floating breakwaters (Giles and Sorensen 1979; Hales 1981)

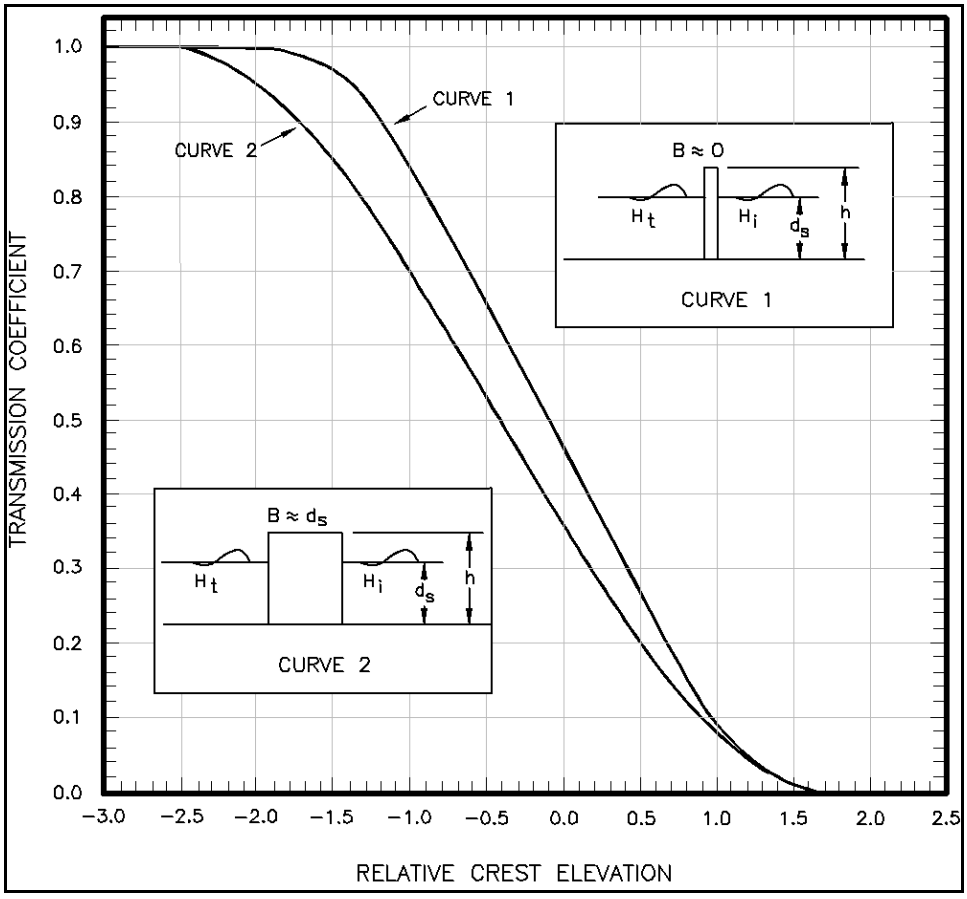

Figure II-7-22. Wave transmission coefficient for vertical wall and vertical thin-wall breakwaters where $0.0157 \le d_s \ \ lgt^2 \le 0.0793$ (based on Goda 2000)

(b) Wave transmission coefficients for a thin and a relatively wide vertical barrier that has its crest above or below the water surface were determined from experiments by Goda (1969). The results, which are for monochromatic waves, are shown in Figure II-7-22. Later tests with irregular waves, where the transmission coefficient is defined in terms of the incident and transmitted significant wave heights, showed that Figure II-7-22 can also be used for irregular wave conditions (Goda 2000). As would be expected, a portion of thetransmitted wave energy shifted to higher frequencies so that the transmitted significant wave period was less than the incident significant period.

(c) Wiegel (1960) developed a simple analytical formulation for wave transmission past a thin rigid vertical barrier that does not extend to the bottom. For monochromatic waves and no overtopping, the resulting transmission coefficient is given by

$$C_t = \left[\frac{\frac{2k(d-y)}{\sinh 2kd} + \frac{\sinh 2k(d-y)}{\sinh 2kd}}{1 + \frac{2kd}{\sinh 2kd}} \right]^{\frac{1}{2}} \tag{II-7-5}$$

where d is the water depth, y is the vertical extent of the barrier below the still-water surface, and $k = 2\pi/L$. In developing Equation II-7-5, Wiegel assumed that the portion of the wave power in the water column below the lower edge of the barrier transmits past the barrier. He used the linear wave theory in this analysis and neglected energy dissipation caused by flow separation at the barrier edge. Limited monochromatic wave tests by Wiegel (1960) and irregular wave tests by Gilman and Nottingham (1992) indicate that Equation II-7-5 can be used for preliminary design calculations.

II-7-4. Wave Reflection

a. Definition of reflection.

(1) If there is a change in water depth as a wave propagates forward, a portion of the wave's energy will be reflected. When a wave hits a vertical, impermeable, rigid surface-piercing wall, essentially all of the wave energy will reflect from the wall. On the other hand, when a wave propagates over a small bottom slope, only a very small portion of the energy will be reflected. The degree of wave reflection is defined by the reflection coefficient $C_r = H_r/H_i$ where H_r and H_i are the reflected and incident wave heights, respectively.

(2) Wave energy that enters a harbor must eventually be dissipated. This dissipation primarily occurs at the harbor interior boundaries. Thus, it is necessary to know the reflection coefficients of the interior boundaries to fully define wave conditions inside a harbor. It may also be necessary, because of excessive wave reflection, to decrease the reflection of certain boundary structures in order to keep interior wave agitation at acceptable levels.

(3) The reflection coefficient for a surface-piercing sloped plane will depend on the slope angle, surface roughness, and porosity. It will also depend on the incident wave steepness H_i/L. Consequently, for a given slope roughness and porosity, the wave reflection will depend on a parameter known as the surf similarity number or Iribarren number (Battjes 1974)

$$I_r = \frac{\tan\alpha}{\sqrt{\frac{H_i}{L_o}}} \tag{II-7-6}$$

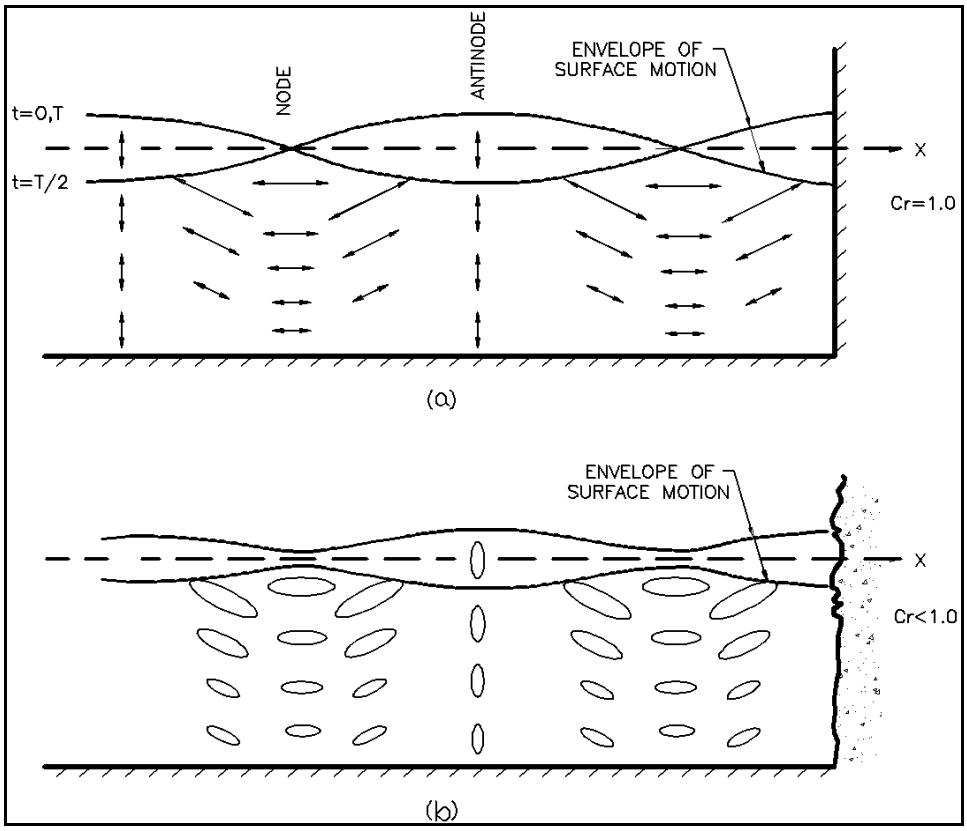

Figure II-7-23. Complete and partial reflection

where α is the angle the slope forms with the horizontal and L_0 is the length of the incident wave in deep water.

(4) Figure II-7-23a is a profile view of the water surface envelope positions for a wave reflecting from a wall that has a reflection coefficient equal to unity (i.e., $H_i = H_r$). The water surface amplitude is given by

$$N = H_i \cos\frac{2\pi x}{L} \cos\frac{2\pi t}{T} \tag{II-7-7}$$

where L and T are the incident and reflected wave length and period respectively, x is the horizontal ordinate and t is the time elapsed. The figure also shows the water particle paths at key points. At nodal points, water particle motions are horizontal and at antinodes, water particle motions are vertical. At $t = 0$, $T/2$, and T, the water is instantaneously still and all of the wave energy is potential energy. At $t = T/4$ and $3T/4$, the water surface is horizontal and all of the energy is kinetic energy.

(5) When the wall reflection coefficient is less than unity, the water surface envelope positions and particle paths are as depicted in Figure II-7-23b. As the reflection coefficient decreases toward zero, the water surface profile and water particle path changes toward the form of a normal progressive wave.

b. Reflection from structures.

(1) Most of the interior boundaries of many harbors are lined with structures such as bulkheads or reveted slopes. Recent laboratory investigations (Seelig and Ahrens 1981; Seelig 1983; Allsop and Hettiarachchi 1988) indicate that the reflection coefficients for most structure forms can be given by the following

$$C_r = \frac{a\, I_r^2}{b + I_r^2} \tag{II-7-8}$$

where the values of coefficients a and b depend primarily on the structure geometry and to a smaller extent on whether waves are monochromatic or irregular. The Iribarren number employs the structure slope and the wave height at the toe of the structure.

(2) Table II-7-1 presents values for the coefficients a and b collected from the above references.

Table II-7-1
Wave Reflection Equation Coefficient Values Structure

Structure	a	b
Plane slope-monochromatic waves	1.0	5.5
Plane slope-irregular waves	1.1	5.7
Rubble-mound breakwaters[1]	0.6	6.6
Dolos-armored breakwaters - monochromatic waves	0.56	10.0
Tetrapod-armored breakwaters - irregular waves	0.48	9.6

[1]This is an average conservative value. Seelig and Ahrens (1981) recommend a range of values for *a* and *b* that depend on the number of stone layers, the relative water depth (*d*/*L*), and the ratio of incident wave height to breaker height.

EXAMPLE PROBLEM II-7-4

FIND:

The height of the reflected wave.

GIVEN:

A wave in deep water has a height of 1.8 m and a period of 6 sec. It propagates toward shore without refracting or diffracting to reflect from a rubble-mound breakwater located in water 5 m deep. The breakwater front slope is 1:1.75 (29.7 deg).

SOLUTION:

From linear wave theory shoaling calculations (Part II-1) the wave height at the structure would be 1.70 m (this is H_i). From the linear wave theory, the deepwater wave length is $L_0 = 56.2$ m. Then, from Equation II-7-6, the Iribarren number is

$$I_r = \frac{\tan 29.7^o}{\sqrt{1.70/56.2}} = 3.28$$

For the coefficient values $a = 0.6$ and $b = 6.6$ (from Table II-7-1), Equation II-7-8 yields

$$C_r = \frac{0.6\,(3.28)^2}{6.6 + (3.28)^2} = 0.37$$

Thus, the reflected wave height $H_r = C_r H_i = 0.37(1.70) = 0.63$ m.

(3) Note that Equation II-7-8 indicates that C_r approaches the value of a at higher values of the Iribarren number. Thus, the highest reflection coefficients for stone and concrete unit armored structures are around 0.5. As expected, vertical plane slopes (infinite Iribarren number) would have a reflection coefficient near unity. For typical rigid vertical bulkheads, owing to the irregularity of the facing surface, a value of $C_r = 0.9$ might be used.

c. Reflection from beaches.

(1) When the reflecting slope becomes very flat, the incident wave will break on the slope, causing an increase in energy dissipation and commensurate decrease in the reflection coefficient. Thus, beaches are generally very efficient wave absorbers, particularly for shorter period wind-generated waves. An added complexity is that as the incident wave conditions change, the beach profile geometry will change, in turn changing the reflection coefficient somewhat. Laboratory measurements of wave reflection from beaches suffer from scale effects in trying to replicate the prototype beach profile, surface roughness, and porosity. Also, it is harder to select a beach slope angle for the Iribarren number owing to the complexity of beach profiles. Thus, data plots follow the form of Equation II-7-8, but with significant scatter in the data points. Seelig and Ahrens (1981) suggest that $a = 0.5$ and $b = 5.5$ be used for beaches. Since the slope angles are small, the Iribarren number will be relatively small, yielding relatively low reflection coefficients.

(2) An interesting phenomenon (known as Bragg reflections after a similar phenomenon in optics) occurs when the shallow nearshore seabed has uniformly spaced bottom undulations. A resonance develops between the incident surface waves of certain periods and the bottom undulations, causing a reflection of a portion of the incident wave energy (see Davies and Heathershaw (1984), Mei (1985), Kirby (1987)). Resonance and reflection are maximum for that portion of the incident wave spectrum having a wavelength that is twice the length of the bottom undulations. There is an approximately linear increase in the reflection coefficient with the increase in the number of bottom undulations. Reflection also increases if the amplitude of the bottom undulations increases or the water depth over the undulations decreases. For appropriate undulation geometries and water depths, reflection coefficients in excess of 0.5 are possible.

(3) It has been suggested (Mei 1985) that Bragg reflections that develop on a nearshore bar system will set up a standing wave pattern seaward of the bar system which, in turn, causes the bar system to extend in the seaward direction. Theoretical, laboratory, and field studies indicate that it is possible to build a series of shore-parallel submerged bars tuned to the dominant incoming wave periods, that will act as a shore protection device. The feasibility of building these bar systems and their economics need to be studied further.

d. Reflection patterns in harbors.

(1) Figure II-7-24 depicts the plan view of a wave crest approaching and reflecting from a barrier that has a reflection coefficient C_r. The incident wave crest is curved owing to refraction and possibly to diffraction. The actual bottom contours in front of the barrier are as shown. The reflected wave crest pattern can be constructed by:

(a) Constructing imaginary mirror image hydrography on the other side of the barrier.

(b) Constructing the wave crest pattern that would develop as the wave propagates over this imaginary hydrography (this would involve the use of refraction and diffraction analyses as described in previous sections).

(c) Constructing the mirror image of the imaginary wave crest pattern to define the real reflected wave.

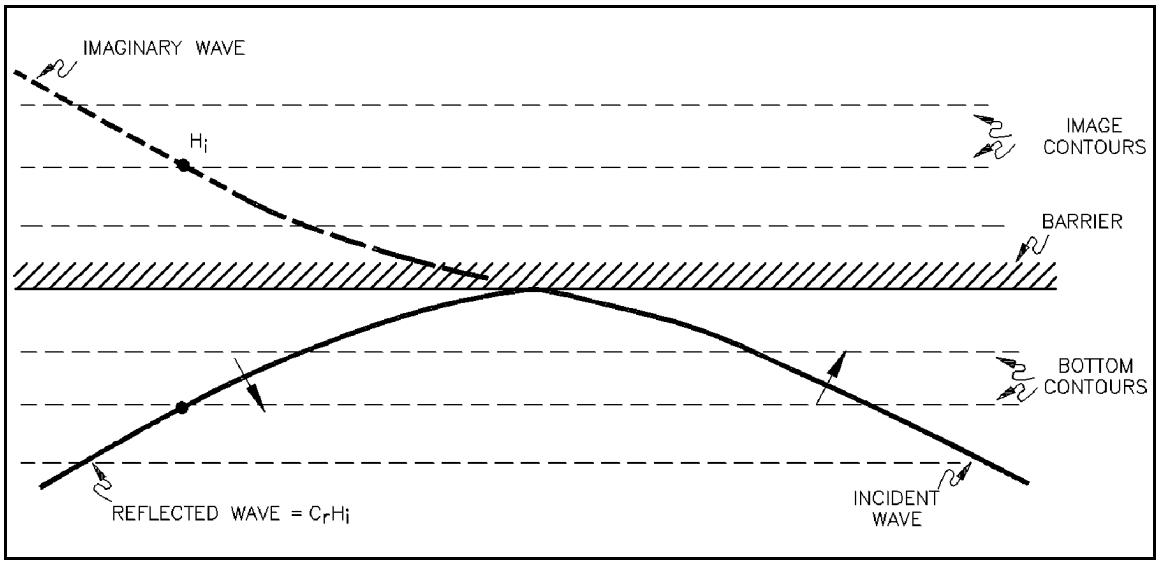

Figure II-7-24. Reflected wave crest pattern

(2) The reflected wave height at any point would be the height at the corresponding point in the imaginary area multiplied by the reflection coefficient at the point on the barrier where that segment of the wave reflected.

(3) Figure II-7-25 shows a wave diffracting in the lee of a breakwater and then reflecting off a wall ($C_r > 0$). The inner end of the reflected wave then hits a beach where it is effectively dissipated; the outer end of the reflected wave diffracts around the breakwater tip and escapes the harbor. The height the reflected wave would have at point A would equal the diffracted height at A' times the reflection coefficient of the wall. By applying the concepts demonstrated in Figures II-7-24 and II-7-25, one can develop the reflection patterns and resulting wave heights for more complex harbor situations (see Carr (1952) and Ippen (1966)).

e. Reflection problems at harbor entrances.

(1) Generally speaking, wave energy that penetrates a harbor entrance should be dissipated as soon as possible, to prevent its subsequent reflection and propagation further into and about the harbor. A number of mechanisms for doing so are discussed in Bruun (1956, 1989). One mechanism is to construct sections of beach, stone mounds or other specially designed wave dissipating structures having low reflection coefficients at appropriate positions just inside the harbor entrance. Another mechanism is to construct resonance chambers at the entrance that are tuned to the dominant frequencies of the incident wave spectrum to set up oscillations that dissipate the penetrating wave energy. Often the general layout of the harbor can be designed to minimize the amount of wave energy that penetrates through the entrance and reflects and rereflects around the harbor.

(2) When significant wave reflection occurs in the vicinity of a harbor entrance (either inside or outside) the incident and reflected waves cross to form a complex “diamond-shaped” wave pattern. Hsu (1990) presents an extensive discussion of the kinematics of the resulting short-crested waves. This form of wave action can cause navigation difficulties and unusual sediment transport and scour patterns (see Silvester and Hsu (1993)).

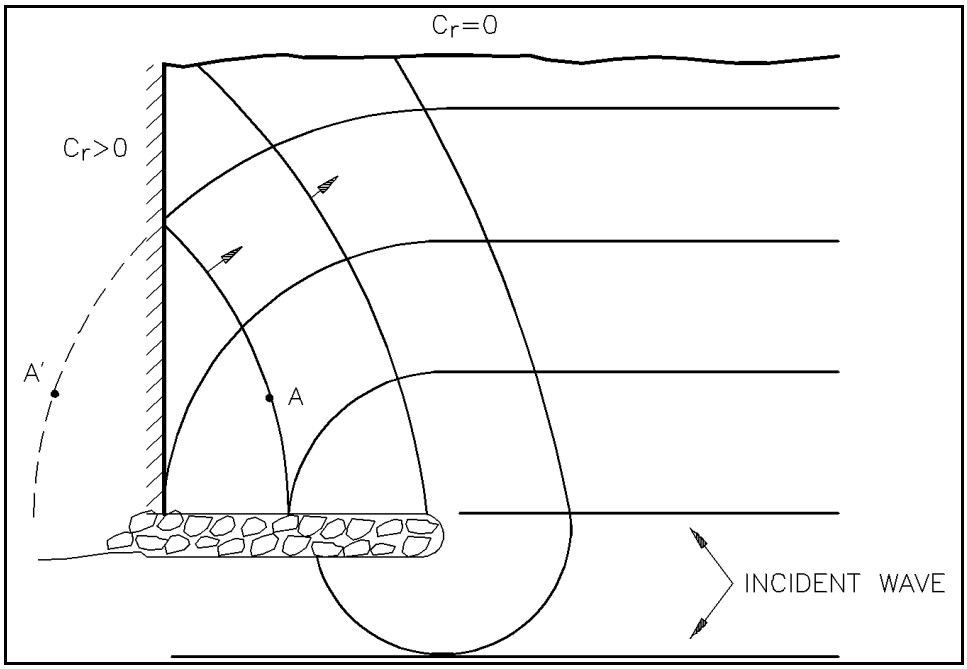

Figure II-7-25. Reflection of a diffracted wave

II-7-5. Harbor Oscillations

a. Introduction.

(1) Harbor oscillations are long-period wave motions that sometimes disrupt harbor activities. The oscillations are standing waves with typical periods between 30 sec and 10 min. Vertical motions are generally small, but horizontal motions can be large. Oscillation characteristics are generally controlled by basin size, shape, and water depth. Oscillations are most damaging when the period coincides with a natural resonant period of the harbor. The phenomenon is also referred to as harbor resonance, surging, seiching, and resonant oscillations.

(2) Harbor oscillations can be a significant problem for inner harbor components and moored vessels within a harbor basin. Resonant periods characteristic of moored vessels often fall into the same range of periods as harbor oscillations. Thus, harbor oscillations can create dangerous mooring conditions including breaking of mooring lines, damage to fender systems, vessel collisions, and delays of loading and unloading operations at port facilities.

(3) Processes and estimation procedures for harbor oscillations are discussed in this section. Discussion of harbor oscillations is generally presented in terms of the characteristics in Table II-7-2.

Table II-7-2
Harbor Oscillation Characteristics

Description	Alternatives	
Basin boundaries	Closed	Open
External forcing	Free	Forced
Dimensionality	2-dimensional	3-dimensional
Basin planform	Simple	Complex

(4) Characteristics are defined as follows:

(a) Closed basin - basin is completely enclosed.

(b) Open basin - basin is semi-enclosed, but open to a larger water body along at least part of one side.

(c) Free oscillations - oscillations that occur without external forcing (although some external forcing was applied earlier to initiate the oscillations).

(d) Forced oscillations - oscillations in response to external forcing.

(e) 2-dimensional - oscillations are independent of one horizontal dimension.

(f) 3-dimensional - oscillations vary in both horizontal dimensions.

(g) Simple - basin planform is a simple geometrical shape, such as a square, rectangle, or circle.

(h) Complex - basin planform is an irregular shape.

(5) A harbor basin generally has several modes of oscillation with corresponding natural resonant frequencies (or periods) and harmonics. Figure II-7-26 illustrates the fundamental, second, and third harmonic modes of oscillation in idealized, perfectly reflecting, closed and open two-dimensional basins.

(6) Following this introduction, the process of resonance is discussed in terms of a more intuitive, but analogous, mechanical system. Closed basins are covered next, mainly in terms of free oscillations and simple shapes. Although they are not closed basins, harbors or parts of harbors can behave much like closed basins under some conditions. The presentation is also applicable to enclosed water bodies such as lakes and reservoirs.

(7) The last parts of the section are devoted to open basins. Open basins are susceptible to oscillations forced across the open boundary. Because of the limited size of harbors, other types of forcing, such as meteorological forcing in the harbor, are generally not considered. Both simple and complex shapes are presented. The final part describes Helmholtz resonance, a very long-period, non-standing wave phenomenon that causes water levels over the entire harbor to oscillate up and down in unison. Practical consequences of harbor oscillation, such as vessel motions, mooring line forces, and fender forces, are not presented in this section. Motions of small boats moored in resonant conditions and possible mitigation measures have been investigated by Raichlen (1968). Comprehensive reviews of harbor oscillations are given by Raichlen and Lee (1992) and Wilson (1972).

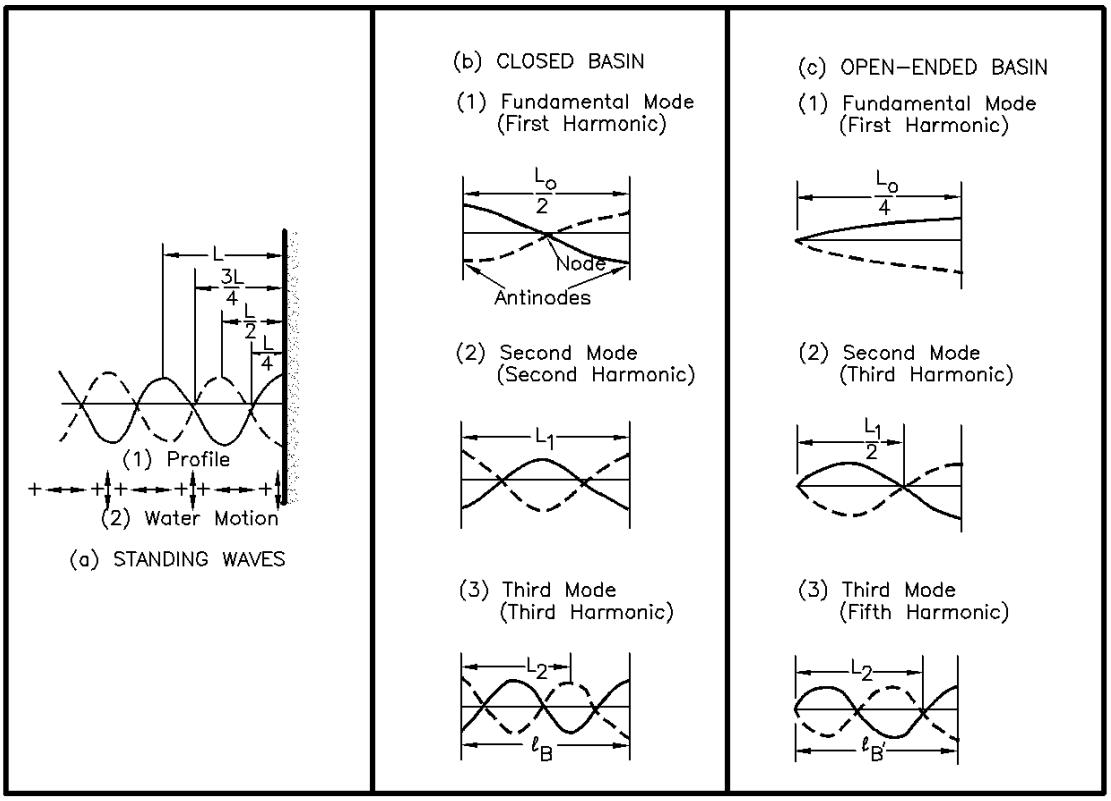

Figure II-7-26. Surface profiles for oscillating waves (Carr 1953)

b. Mechanical analogy.

(1) The basic theory for basin oscillations is similar to that of free and forced oscillations experienced by some mechanical, acoustical, and other fluid systems. Certain systems respond to a disturbance by developing a restoring force that reestablishes equilibrium in the system. A pendulum is a good example of such a system. A free oscillation at the system's natural period or frequency is initiated if the system is carried by inertia beyond the equilibrium condition. If the forces responsible for the initial disturbance are not sustained, free oscillations at the natural frequency will continue, but their amplitude decays exponentially due to friction. The system eventually comes to rest. Forced oscillations can occur at non-natural frequencies if cyclic energy is applied to a system at non-natural frequencies. Continuous excitation at frequencies at or near the natural frequency of a system generally causes an amplified response. The response magnitude depends on the proximity of the excitation to the natural frequency and the frictional characteristics of the system.

(2) The response of a linearly damped, vibrating spring-mass system with one degree of freedom provides a good illustration (Figure II-7-27). Terms are defined as follows: A = amplification factor (ratio of mass displacement to excitation displacement); T = excitation (and response) period; T_n = natural period of the mass-spring system; and φ = phase angle by which the mass displacement lags the excitation displacement. The mass responds directly to the excitation if the excitation period is much greater than the natural period of the system; that is, $A = 1$ and $\varphi = 0°$ when $T_n/T << 1$. The harbor equivalence to this case is the harbor response to astronomical tides. The mass responds very little and out of phase with the excitation if the excitation period is much shorter than the natural period of the system; that is, $A << 1$ and $\varphi \simeq 180°$ when $T_n/T >> 1$. The mass response is amplified and a phase lag develops as the excitation period approaches the natural period of the system. The ratio T_n/T determines the degree of amplification and phase

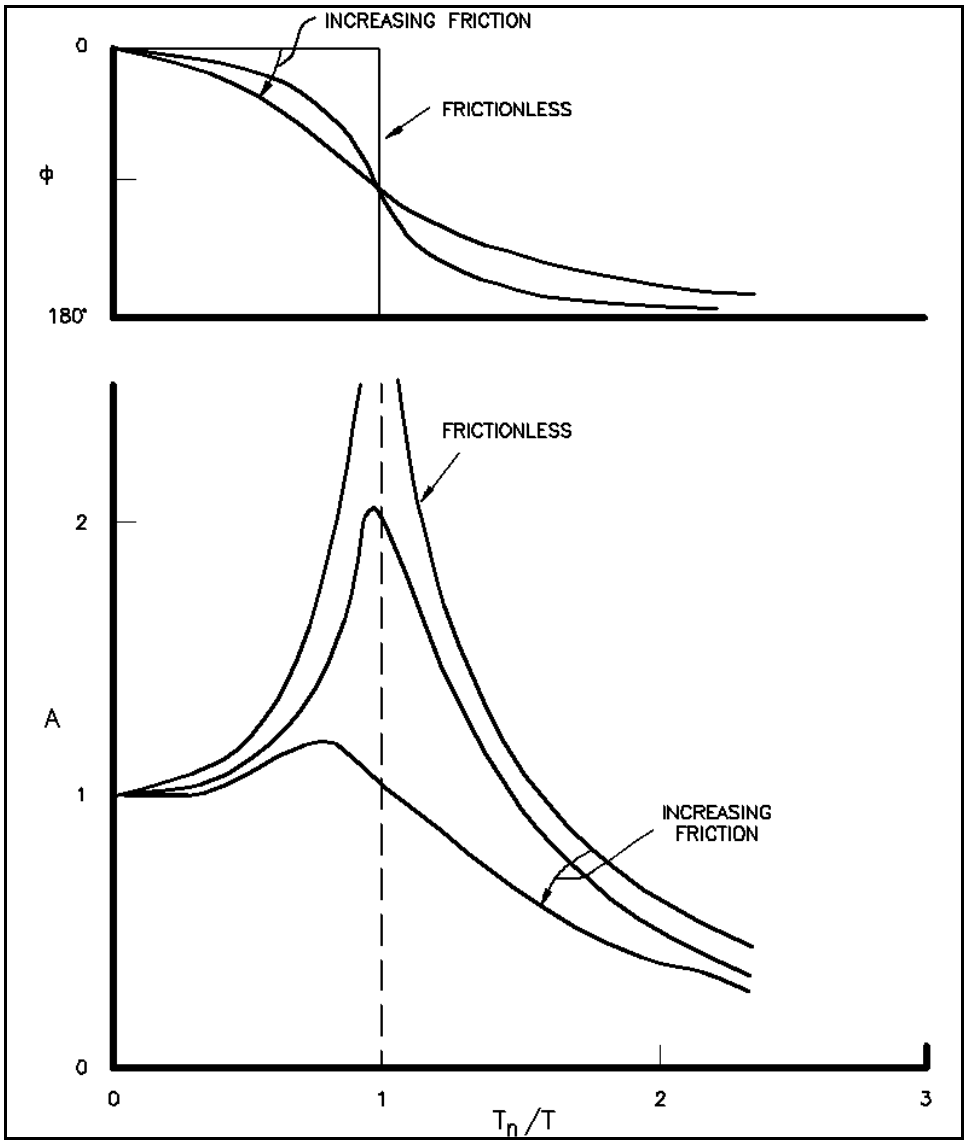

Figure II-7-27. Behavior of an oscillating system with one degree of freedom

lag. The greatest amplification occurs when $T_n/T = 1$ and $\varphi = 90$ deg. With a cyclic excitation at period T_n, the amplification factor increases with time until the rate of energy input equals the rate of energy dissipation by friction. When energy input is stopped, the response amplitude decreases exponentially with time as a result of friction. Amplification due to resonance in a mass-spring system and the respective phase relationships are further developed and discussed in Raichlen (1968), Meirovitch (1975), Sorensen (1986), and Wilson (1972).

c. Closed basins.

(1) Enclosed basins can experience oscillations due to a variety of causes. Lake oscillations are usually the result of a sudden change, or a series of intermittent-periodic changes, in atmospheric pressure or wind velocity. Oscillations in canals can be initiated by suddenly adding or subtracting large quantities of water. Harbor oscillations are usually initiated by forcing through the entrance; hence, they deviate from a true closed basin. Local seismic activity can also create oscillations in an enclosed basin.